

NASA MEMO 11-26-58E

CASE FILE  
COPY

11-07  
394 519

APR 17 1959

# NASA

## MEMORANDUM

COMPARISON OF CALCULATED AND EXPERIMENTAL TOTAL-  
PRESSURE LOSS AND AIRFLOW DISTRIBUTION IN TUBULAR  
TURBOJET COMBUSTORS WITH TAPERED LINERS

By Jack S. Grobman

Lewis Research Center  
Cleveland, Ohio

PROPERLY FILED  
ENGINEERING LIBRARY

# NATIONAL AERONAUTICS AND SPACE ADMINISTRATION

WASHINGTON

January 1959

AK

8



NATIONAL AERONAUTICS AND SPACE ADMINISTRATION

MEMORANDUM 11-26-58E

COMPARISON OF CALCULATED AND EXPERIMENTAL TOTAL-PRESSURE

LOSS AND AIRFLOW DISTRIBUTION IN TUBULAR TURBOJET

COMBUSTORS WITH TAPERED LINERS

By Jack S. Grobman

SUMMARY

Incompressible-flow calculations were performed to determine the effects of combustor geometric and operating variables on pressure loss and airflow distribution in a tubular combustor with a tapered liner. The calculations include the effects of momentum transfer between annulus and liner gas streams, annulus wall friction, heat release, and discharge coefficients of liner air-entry holes. Generalized curves are presented which show the effects of liner-wall inclination, liner open hole area, and temperature rise across the combustor on pressure loss and airflow distribution for a representative parabolic liner hole distribution. A comparison of the experimental data from 12 tapered liners with the theoretical calculations indicates that reasonable design estimates can be made from the generalized curves. The calculated pressure losses of the tapered liners are compared with those previously reported for tubular liners.

INTRODUCTION

Knowledge of the total-pressure loss and airflow distribution are important considerations in the design of combustors for turbojet or ram-jet engines. A loss in the total pressure of the gases flowing through a combustor reduces engine thrust and cycle efficiency, while the axial distribution of air along the combustor liner may markedly affect combustor performance. A theoretical analysis of total-pressure loss and liner airflow distribution for parallel-walled combustors is presented in reference 1. A comparison of the theoretical analysis of reference 1 with unpublished experimental data indicated that reasonable design estimates could be made from the calculated data. The present report, which is an extension of the previous work, presents both theoretical and experimental data for a tapered combustor liner.

The total-pressure losses in a combustor are mainly attributed to the following flow phenomena, which are considered in the present analysis: (1) momentum transfer between high-velocity liner air jets and the liner gas stream, (2) heat release, and (3) skin friction. The theoretical curves in this report present total-pressure loss and airflow distribution as a function of the following dimensionless parameters: (1) liner-wall inclination, (2) ratio of combustor length to combustor reference diameter, (3) ratio of liner cross-sectional area upstream of first air-entry holes to combustor reference area, where the combustor reference area is defined as the total combustor cross-sectional area, (4) ratio of total liner open hole area to combustor reference area, and (5) ratio of combustor-exit to inlet total temperature.

The calculated total-pressure-loss data are compared with experimental data obtained with 12 tapered liner configurations operating over a range of flow conditions. Isothermal total-pressure-loss data were obtained for all configurations, while limited data for total-pressure loss were obtained with heat release. In addition, isothermal liner airflow distribution data were obtained for a single tapered liner.

#### ANALYSIS

The analysis for the tapered combustor liner used in this report was developed from the equations of reference 1 by negating the assumption of constant annulus and liner cross-sectional area. A diagram of the combustor with a tapered liner is shown in figure 1. (The symbols used in this report are defined in appendix A.)

The derivations of the incompressible-flow equations used in this report are given in appendix B. The assumptions are the same as those given in reference 1 except that liner and annulus cross-sectional areas are variable over the length of the combustor. The principal assumptions used in the derivation of the equations are:

- (1) The actual flow can be approximated with sufficient accuracy by one-dimensional equations.
- (2) The liner air jets mix instantaneously with the liner gas stream.
- (3) The effects of fuel flow on molecular weight and weight flow of the liner gas stream can be neglected.
- (4) Heat transfer between the annulus and liner gas streams is negligible.
- (5) Mixing losses in the annulus are negligible.
- (6) Liner wall friction is negligible.

(7) Density is independent of pressure changes along the combustor and is affected only by the temperature changes due to heat release.

The evaluation of  $T_L$  with combustion would require knowledge of the fuel-air ratio and the average combustion efficiency along the combustor. In typical combustors, the major portion of the inlet air is bypassed around the liner dome, where all the fuel is injected. Accordingly, the average fuel-air ratio of the liner gas stream may vary from values well in excess of stoichiometric at the upstream end of the combustor to lean values at the combustor exit. If all the fuel is injected at the liner dome, the average fuel-air ratio of the liner gas stream at various stations along the combustor  $F_L$  is given by

$$F_L = \frac{F_{L,3}}{w_L/w_T} \quad (1)$$

where  $F_{L,3}$  is the over-all fuel-air ratio of the combustor.

In the present calculations, the combustion efficiency was assumed to be 100 percent in the downstream portion of the combustor, where the average fuel-air ratio of the liner gas stream is stoichiometric or leaner. In the upstream portion of the combustor, where the overrich fuel-air ratios exist, the average temperature of the liner gas stream was assumed to be that corresponding to a stoichiometric fuel-air ratio and 100-percent combustion efficiency. The value of  $T_L/T_1$  along the combustor for various values of  $w_L/w_T$  was calculated as in reference 1 from the chosen value of  $T_{L,3}/T_1$  and the curve for the variation of  $T_L/T_1$  with fuel-air ratio (fig. 2).

#### Combustor Total-Pressure-Loss Coefficient

As shown in appendix B, the relation between the total open hole area of the liner and the flow conditions along the liner can be expressed as follows:

$$\frac{A_{h,T}}{A_r} = \int_{\frac{w_{L,2}}{w_T}}^1 \frac{d\left(\frac{w_L}{w_T}\right)}{C \sqrt{\frac{(P_A - P_L)}{q_r}} \left[ 1 + \frac{q_A \sin \alpha}{(P_A - P_L)} \right]} \quad (2)$$

E-126

CQ-1 back

In equation (2) the annulus total pressure  $P_A$  may be calculated from the combustor-inlet total pressure and the friction pressure drop along the annulus, while the liner static pressure  $p_L$  may be calculated from the momentum equation for the liner gas stream, as shown in appendix B. When the annulus and liner cross-sectional areas are variable along the combustor, the term  $(P_A - p_L)/q_r$  of equation (2) is related to the combustor total-pressure-loss coefficient  $\Delta P/q_r$  by

$$\frac{P_A - p_L}{q_r} = \frac{\Delta P}{q_r} - \frac{P_L - P_A}{q_r} - 2 \int_1^{w_L/w_T} \left(1 - \frac{w_L}{w_T}\right) \left(\frac{A_r}{A_A}\right) \left(\frac{A_r}{A_L}\right) d\left(\frac{w_L}{w_T}\right) +$$

$$2 \int_{\left(\frac{T_{L,3}}{T_1}\right)}^{\left(\frac{w_L}{w_T}\right)^2 \left(\frac{T_L}{T_1}\right) \left(\frac{A_r}{A_L}\right)} \left(\frac{A_r}{A_L}\right) d\left[\left(\frac{w_L}{w_T}\right)^2 \left(\frac{T_L}{T_1}\right) \left(\frac{A_r}{A_L}\right)\right] + \frac{T_{L,3}}{T_1} \quad (3)$$

The relation between  $\Delta P/q_r$  and  $A_{h,T}/A_r$  is obtained from the solutions of equations (2) and (3). The equations are solved using graphical or trapezoidal integration. A value of  $A_{h,T}/A_r$  is obtained for specified values of  $\Delta P/q_r$ ,  $L/D$ ,  $\alpha$ ,  $T_{L,3}/T_1$ , and the specified airflow distribution along the combustor.

#### Airflow Distribution

The liner airflow distribution is obtained as shown in appendix B from the relation

$$\frac{A_h}{A_{h,T}} = \frac{\int_{\frac{w_{L,2}}{w_T}}^{\frac{w_L}{w_T}} \frac{d\left(\frac{w_L}{w_T}\right)}{C \sqrt{\frac{P_A - p_L}{q_r} \left(1 + \frac{q_A \sin \alpha}{P_A - p_L}\right)}}}{\int_{\frac{w_{L,2}}{w_T}}^1 \frac{d\left(\frac{w_L}{w_T}\right)}{C \sqrt{\frac{P_A - p_L}{q_r} \left(1 + \frac{q_A \sin \alpha}{P_A - p_L}\right)}}} \quad (4)$$

From equation (4), values for the fractional liner open hole area  $A_h/A_{h,T}$  may be calculated for various values of  $w_L/w_T$ .

### Orifice Discharge Coefficient

All calculations presented herein are based on discharge coefficients for 3/4-inch-diameter air-entry holes, a 0.04-inch-thick wall, and parallel crossflow ( $\alpha = 0$ ). This simplification was made because references 2 and 3 show the effects of hole size, wall thickness, and wall inclination to be quite small compared to the effect of the flow parameter  $(P_A - p_j)/(P_A - p_A)$  shown in figure 3.

## APPARATUS AND PROCEDURE

### Combustor Installation

A schematic diagram of the research combustor installation is shown in figure 4. The combustor was connected to the laboratory pressurized air and exhaust systems. The airflow rate and combustor pressure were regulated by remotely controlled valves. Airflow was metered by a calibrated flow nozzle having a throat diameter of 4.543 inches (station A, fig. 4).

An 8.0-inch-inner-diameter housing was used for all tests. Each of the liners was welded at the exhaust end to a support ring which was positioned between the flanges of the combustor housing and the instrument ducting. The dimensions of the liner models studied are given in table I. Each liner was made of 0.043-inch Inconel and had 108 air-entry holes spaced so as to give the parabolic liner hole area distribution shown in figure 5. In the calculations, values for the liner hole distribution were obtained from the faired curve rather than the step curve shown in figure 5. The liner open hole area of each configuration was varied by changing hole diameter from 1/2 to 5/8 to 3/4 inch. All openings were flush circular holes, and there was no airflow through the liner dome. For tests with heat release, a fuel nozzle supplying gaseous propane and an ignition plug were installed in the dome of the liner. Fuel flow was metered by a square-edged orifice with a 0.750-inch diameter.

### Instrumentation

Total-pressure surveys upstream and downstream of the combustor (stations B and C, fig. 4) were made with 20 total-pressure tubes per station, the tubes being located along centerlines of five equal areas. Combustor-inlet air temperature was measured by iron-constantan

thermocouples. For tests with heat release in the combustor, 32 Chromel-Alumel thermocouples (equally spaced along the centerlines of four equal areas) were installed at station D immediately downstream of the pressure-measuring station C (fig. 4). Experimental static-pressure distribution data were obtained with one combustor configuration (model D, table I), which was equipped with liner and annulus static-pressure taps at each row of air-entry holes.

### Procedure

Experimental pressure-loss data were obtained for all 12 liner configurations at isothermal flow conditions. The inlet air temperature was approximately 80° F for all tests. All test data were obtained at constant nominal airflows of 2 and 4 pounds per second; combustor-inlet pressure was varied from about 10 to 60 inches of mercury absolute to give a range of reference Mach numbers of about 0.04 to 0.25. Limited pressure-loss data with heat release were obtained for five configurations. Heat-release data were obtained at average exhaust temperatures of about 2 to 4 times the inlet absolute temperature.

### RESULTS AND DISCUSSION

Results presented in reference 1 concern the pressure loss and air-flow distribution of parallel-walled combustors. The results presented herein pertain to tubular combustors with tapered liners. In the analysis of the parallel-walled combustor (ref. 1), the variation of the fractional airflow  $w_L/w_T$  with distance  $x$  along the liner was important only in the consideration of the annulus wall friction. The variation of the fractional airflow with distance along the liner has added significance in the tubular combustor with a tapered liner because, since the liner cross-sectional area is not constant, an additional variable is added to the momentum equation for the liner gas stream.

The calculations herein were based on the axial airflow distribution shown in figure 6. The same axial airflow distribution was used in the calculations of reference 1. This airflow distribution was assumed to correspond to the experimental liner hole area distribution shown in figure 5 because preliminary calculations indicated that the variation in the orifice discharge coefficient along tapered liners is small for the range of liner open hole area considered in the experimental tests.

### Combustor Total-Pressure Loss

Calculated combustor total-pressure-loss coefficient. - Figure 7 shows the effect of the ratio of liner total open hole area to combustor



reference area  $A_{h,T}/A_r$  on the combustor total-pressure-loss coefficient  $\Delta P/q_r$  for various values of  $L/D$ ,  $\alpha$ , and  $T_{L,3}/T_1$ . Total-pressure loss was calculated for the largest liner total open hole area for which the static-pressure drop across any given air-entry station was as low as the reference dynamic pressure  $q_r$ . Further increases in liner total open hole area from this value would be expected to give only small reductions in the total-pressure-loss coefficient and possible reverse flow from the liner gas stream to the annulus stream. Decreasing  $A_{h,T}/A_r$  below a value of about 0.6 results in a rapid increase in  $\Delta P/q_r$ . Analogous results are given in reference 1 for the cylindrical liner.

Increasing  $L/D$  for a given value of  $\alpha$  decreases  $\Delta P/q_r$ , while increasing  $\alpha$  for a given value of  $L/D$  causes  $\Delta P/q_r$  to pass through a minimum. The combined effect of  $L/D$  and  $\alpha$  can be demonstrated by relating these two variables to the ratio of liner cross-sectional area at station 2 to combustor reference area  $A_{L,2}/A_r$  as shown in figure 8. The pressure-loss data of figure 7 are cross-plotted in figure 9 as a function of  $A_{L,2}/A_r$  for values of  $A_{h,T}/A_r$  of 0.6 and 1.0 and for values of  $T_{L,3}/T_1$  of 1, 2, 3, and 4. The effect of annulus wall friction for increasing values of  $L/D$  had only a minor effect on  $\Delta P/q_r$  for the conditions specified in the figure; therefore, a single curve is shown for the range of  $L/D$  studied. For a given value of  $A_{h,T}/A_r$ , the isothermal total-pressure-loss coefficient increases parabolically as  $A_{L,2}/A_r$  is increased. The minimum of the parabolic curve shifts to higher values of  $A_{L,2}/A_r$  as  $T_{L,3}/T_1$  is increased. Comparative data for the cylindrical liner from reference 1 are also presented in figure 9. Both sets of data display a shift of the minimum total-pressure-loss coefficient to higher values of  $A_{L,2}/A_r$  as the temperature ratio is increased. At a value of  $T_{L,3}/T_1$  of 3, the minimum value of  $\Delta P/q_r$  occurs at a value of  $A_{L,2}/A_r$  of 0.6 for the cylindrical liner and at a value of  $A_{L,2}/A_r$  of approximately 0.3 for the tapered liner.

The calculated isothermal total-pressure-loss coefficient for the tapered liner and the cylindrical liner (ref. 1) are compared in figure 10. The total-pressure-loss coefficient is plotted against  $A_{h,T}/A_r$  for various values of  $A_{L,2}/A_r$ . The tapered liner gives lower pressure losses than the cylindrical liner for values of  $A_{L,2}/A_r$  of 0.4 and below for isothermal flow. The total-pressure-loss coefficient is lower for a tapered liner than for a cylindrical liner for values of  $A_{L,2}/A_r$  of 0.6 and below for a value of  $T_{L,3}/T_1$  of 4 (fig. 9).

Experimental combustor total-pressure-loss coefficient. - The isothermal total-pressure-loss data for 12 experimental liners are shown in figure 11. The total-pressure-loss coefficient is plotted against reference Mach number  $M_r$  for nominal airflow rates of 2 and 4 pounds per second. Limited data with heat release are also shown for five liner configurations (figs. 11(c), (f), (i), (k), and (l)). The increase in total-pressure-loss coefficient with increasing reference Mach number is similar to that shown by unpublished experimental data for cylindrical liners and predicted by the compressible-flow calculations of reference 1. The isothermal total-pressure-loss data for the 12 tapered liners are compared in figure 12. The rate of increase in total-pressure-loss coefficient with reference Mach number is less pronounced for the low-pressure-loss configurations.

The isothermal total-pressure-loss data for the 12 liners are compared with the calculated incompressible-flow data in figure 13. Since the calculated data are based on incompressible-flow relations, they are comparable with the experimental data only for low reference Mach numbers. In general, in this low  $M_r$  region, the calculated value of the total-pressure-loss coefficient exceeds the experimental value by about 10 to 40 percent; however, for model C (fig. 13(c)) the calculated data varied from the experimental data by  $\pm 10$  percent. A compressible-flow analysis for tapered liners similar to that developed for the cylindrical liner in reference 1 could account for the variation in total-pressure-loss coefficient with reference Mach number.

A comparison of the experimental and calculated total-pressure-loss coefficients for several liner configurations with heat release is shown in figure 14. With the exception of model A (fig. 14(a)), the experimental total-pressure-loss coefficient increased with a greater slope than the calculated values as the temperature ratio was increased. Combustion instability and flame ejection through upstream liner openings was observed for some of the tests and could account for higher values of  $\Delta P/q_r$ . In addition, combustion was limited to a narrow operating range because combustion inefficiency and flame blowout resulted as the combustion pressure was lowered, as indicated by increasing  $V_r/P_1 T_1$  in figure 15.

#### Combustor-Liner Airflow Distribution

Calculated airflow distribution. - The variation of the fractional airflow distribution along the liner with  $A_h/A_{h,T}$  for values of  $A_{h,T}/A_r$  of 0.6 and 1.0 and values of  $T_{L,3}/T_1$  of 1 and 4 is shown in figure 16. Data are shown for values of  $A_{L,2}/A_r$  of 0.3, 0.4, and 0.5. Independent curves showing the effects of  $L/D$  and  $\alpha$  are not presented

because the calculations indicated that these variables have negligible effects compared to that shown by  $A_{L,2}/A_r$ . Increasing  $A_{h,T}/A_r$  or  $T_{L,3}/T_1$  tends to decrease the fraction of air entering the upstream portion of the liner. Similar results are presented for the cylindrical liner in reference 1. This reduction in upstream liner airflow becomes more severe as the value of  $A_{L,2}/A_r$  is reduced.

Experimental airflow distribution. - Limited experimental data for one tapered and one cylindrical liner configuration are compared with calculated airflow distribution data in figure 17. The experimental airflow distribution for the cylindrical liner shown is from unpublished NACA data, and the calculated cylindrical airflow distribution is from reference 1. The experimental data shown were computed from measured static-pressure drop across the air-entry stations along the liner and the discharge-coefficient data of reference 2. Reasonable agreement between experimental and calculated data is shown in the figure.

#### SUMMARY OF RESULTS

The effects of a number of geometric and operating variables on total-pressure loss and airflow distribution were determined from incompressible-flow relations for a tapered combustor liner. The results of these calculations were compared with both experimental tapered-liner data and calculated data reported previously for a cylindrical liner. The following conclusions were reached for a tapered liner with a parabolic axial airflow distribution:

1. The minimum calculated total-pressure-loss coefficient for a given total open hole area occurs at a ratio of liner cross-sectional area upstream of the first air-entry holes to reference area  $A_{L,2}/A_r$  of 0.1 for isothermal flow and at a value of  $A_{L,2}/A_r$  of 0.3 for a temperature ratio across the combustor of 4.

2. For a given liner total open hole area, the calculated total-pressure-loss coefficient of the tapered liner is lower than that for a cylindrical liner when  $A_{L,2}/A_r$  is below about 0.4 for isothermal flow and when  $A_{L,2}/A_r$  is below about 0.6 for a temperature ratio of 4.

3. The calculated total-pressure-loss coefficient generally exceeded the experimental value by 10 to 40 percent for isothermal flow.

4. With heat release in the combustor the experimental total-pressure-loss coefficient generally increased at a faster rate with the temperature

ratio across the combustor than the calculated value and exceeded the calculated value by about 10 percent at a temperature ratio of 4.

Lewis Research Center  
National Aeronautics and Space Administration  
Cleveland, Ohio, September 2, 1958

## APPENDIX A

## SYMBOLS

The symbols used in this report are as follows:

A	cross-sectional area of any given flow passage, sq ft
A <sub>A</sub>	cross-sectional area of annulus at any given station formed by outer diameter of liner d and inner diameter of combustor housing D, sq ft
A <sub>h</sub>	liner open hole area from station 2 to station x, sq ft
A <sub>h,T</sub>	total open hole area in liner wall (excluding liner dome openings), sq ft
A <sub>L</sub>	cross-sectional area of liner at any given station, sq ft
A <sub>r</sub>	total combustor cross-sectional area, reference area, $(\pi/4) D^2$ , sq ft
C	orifice discharge coefficient, ratio of measured to theoretical flow through hole
C <sub>p</sub>	orifice discharge coefficient corrected for pressure-ratio effect
D	inner diameter of combustor housing, reference diameter, ft
d	outer diameter of liner, ft
F	fuel-air ratio by weight
f	Fanning friction factor
g	gravitational constant, 32.2 ft/sec <sup>2</sup>
L	length of combustor from station 2 to vertex formed by downstream end of liner wall and combustor shell
l	length of combustor from station 2, just upstream of first row of holes in liner, to station 3, downstream of last row of holes in liner
M	Mach number based on local average velocity and local static temperature
P	local total pressure, lb/sq ft

$\Delta P/q_r$	combustor total-pressure-loss coefficient
$p$	local static pressure, lb/sq ft
$q$	dynamic pressure, lb/sq ft
$q_r$	reference dynamic pressure, $w_T^2/2g\rho_1 A_r^2$ , lb/sq ft
$r$	hydraulic radius, ft
$T$	local total temperature, °R
$V$	local average velocity, ft/sec
$w$	weight-flow rate of air passing through any given flow passage, lb/sec
$w_L$	weight-flow rate of air passing through liner at given station, lb/sec
$w_T$	total weight-flow rate of air passing through combustor, lb/sec
$x$	distance along combustor measured from station 2, just upstream of first holes in liner, ft
$\alpha$	angle of inclination of liner wall, deg
$\rho$	density based on static pressure and static temperature, lb/cu ft

## Subscripts:

A	annulus
J	jet issuing from liner wall opening
L	liner
n	normal to hole
r	reference
1	combustor inlet
2	station just upstream of first liner wall opening
3	combustor-exit station, downstream of last liner wall opening

## APPENDIX B

## INCOMPRESSIBLE-FLOW CALCULATIONS FOR TUBULAR TURBOJET

## COMBUSTORS WITH TAPERED LINERS

The flow equation for a differential portion of air passing through a liner wall opening may be written as

$$dw_L = C \rho_j V_j dA_h \quad (B1)$$

or as

$$dw_L = C_n \rho_j V_n dA_h \quad (B2)$$

where

$$V_j^2 = V_n^2 + V_A^2 \quad (B3)$$

The relation between  $C$  and  $C_n$  is then

$$C = C_n \sqrt{\frac{(P_A - P_L)}{(P_A - P_L)}} \quad (B4)$$

for incompressible flow. The flow equation (B2) for a tapered combustor with a wall angle  $\alpha$  can be written as

$$d\left(\frac{w_L}{w_T}\right) = C_n \sqrt{\frac{(P_A - P_L)}{q_r} + \frac{q_A}{q_r} \sin \alpha} d\left(\frac{A_h}{A_r}\right) \quad (B5)$$

For convenience equation (B5) was converted as follows by substitution of equation (B4) to accommodate the use of the discharge coefficient  $C$ :

$$d\left(\frac{w_L}{w_T}\right) = C \sqrt{\frac{(P_A - P_L)}{q_r} \left[1 + \frac{q_A \sin \alpha}{(P_A - P_L)}\right]} d\left(\frac{A_h}{A_r}\right) \quad (B6)$$

Equation (B6) can be numerically integrated to obtain relations for  $A_{h,T}/A_r$  and  $A_h/A_{h,T}$  for various values of  $w_L/w_T$ :

$$\frac{A_{h,T}}{A_r} = \int_{\frac{w_{L,2}}{w_T}}^1 \frac{d\left(\frac{w_L}{w_T}\right)}{c \sqrt{\frac{(p_A - p_L)}{q_r} \left[1 + \frac{q_A \sin \alpha}{(p_A - p_L)}\right]}} \quad (2)$$

and

$$\frac{A_h}{A_{h,T}} = \frac{\int_{\frac{w_{L,2}}{w_T}}^{\frac{w_L}{w_T}} \frac{d\left(\frac{w_L}{w_T}\right)}{c \sqrt{\frac{p_A - p_L}{q_r} \left(1 + \frac{q_A \sin \alpha}{p_A - p_L}\right)}}}{\int_{\frac{w_{L,2}}{w_T}}^1 \frac{d\left(\frac{w_L}{w_T}\right)}{c \sqrt{\frac{p_A - p_L}{q_r} \left(1 + \frac{q_A \sin \alpha}{p_A - p_L}\right)}}} \quad (4)$$

The differential momentum equation for the liner as developed in reference 1 is

$$A_L dp_L + \frac{w_L}{g} dv_L + \frac{V_L}{g} dw_L - \frac{V_A}{g} dw_L = 0 \quad (B7)$$

Introducing the dynamic pressure term makes the equation dimensionless:

$$dp_L + 2q_r \left(\frac{A_r}{A_L}\right) d\left[\left(\frac{w_L}{w_T}\right)^2 \left(\frac{T_L}{T_1}\right) \left(\frac{A_r}{A_L}\right)\right] - 2q_r \left(1 - \frac{w_L}{w_T}\right) \left(\frac{A_r}{A_A}\right) \left(\frac{A_r}{A_L}\right) d\left(\frac{w_L}{w_T}\right) = 0 \quad (B8)$$



Integrating equation (B8) from station 3 (fig. 1) to station x results in

$$\int_{p_{L,3}}^{p_L} dp_L + 2q_r \int_{\left(\frac{T_{L,3}}{T_1}\right)}^{\left(\frac{w_L}{w_T}\right)^2 \left(\frac{T_L}{T_1}\right) \left(\frac{A_r}{A_L}\right)} \left(\frac{A_r}{A_L}\right) d \left[ \left(\frac{w_L}{w_T}\right)^2 \left(\frac{T_L}{T_1}\right) \left(\frac{A_r}{A_L}\right) \right] -$$

$$2q_r \int_1^{\left(\frac{w_L}{w_T}\right)} \left(\frac{A_r}{A_A}\right) \left(\frac{A_r}{A_L}\right) \left(1 - \frac{w_L}{w_T}\right) d \left(\frac{w_L}{w_T}\right) = 0 \quad (B9)$$

where  $\frac{A_r}{A_{L,3}} = 1$ , assuming  $A_L + A_A = A_r = \text{Constant}$ . Then

$$\frac{(p_L - p_{L,3})}{q_r} = 2 \int_1^{\left(\frac{w_L}{w_T}\right)} \left(1 - \frac{w_L}{w_T}\right) \left(\frac{A_r}{A_A}\right) \left(\frac{A_r}{A_L}\right) d \left(\frac{w_L}{w_T}\right) -$$

$$2 \int_{\left(\frac{T_{L,3}}{T_1}\right)}^{\left(\frac{w_L}{w_T}\right)^2 \left(\frac{T_L}{T_1}\right) \left(\frac{A_r}{A_L}\right)} \left(\frac{A_r}{A_L}\right) d \left[ \left(\frac{w_L}{w_T}\right)^2 \left(\frac{T_L}{T_1}\right) \left(\frac{A_r}{A_L}\right) \right] \quad (B10)$$

Equation (B10) can be used to find a solution for the pressure term in equations (2) and (4) as follows:

$$\frac{(p_A - p_L)}{q_r} = \frac{(p_1 - p_L)}{q_r} - \frac{(p_1 - p_A)}{q_r}$$

$$= \frac{(p_1 - p_{L,3})}{q_r} - \frac{(p_1 - p_A)}{q_r} - \frac{(p_L - p_{L,3})}{q_r} + \frac{q_{L,3}}{q_r} \quad (B11)$$

Equation (B11) can be written

$$\frac{P_A - P_L}{q_r} = \frac{\Delta P}{q_r} - \frac{P_1 - P_A}{q_r} - 2 \int_1^{w_L/w_T} \left(1 - \frac{w_L}{w_T}\right) \left(\frac{A_r}{A_A}\right) \left(\frac{A_r}{A_L}\right) d\left(\frac{w_L}{w_T}\right) +$$

$$2 \int \left(\frac{w_L}{w_T}\right)^2 \left(\frac{T_L}{T_1}\right) \left(\frac{A_r}{A_L}\right) \left(\frac{A_r}{A_L}\right) d\left[\left(\frac{w_L}{w_T}\right)^2 \left(\frac{T_L}{T_1}\right) \left(\frac{A_r}{A_L}\right)\right] + \left(\frac{T_{L,3}}{T_1}\right)$$

$$\left(\frac{T_{L,3}}{T_1}\right) \quad (3)$$

The term  $\frac{q_A}{(P_A - P_L)}$  in equations (2) and (4) can be calculated as follows:

$$\frac{q_A}{(P_A - P_L)} = \frac{\frac{q_A}{q_r}}{\frac{(P_A - P_L)}{q_r} - \frac{q_A}{q_r}} = \frac{\left(\frac{A_r}{A_A}\right)^2 \left(1 - \frac{w_L}{w_T}\right)^2}{\left(\frac{P_A - P_L}{q_r}\right) - \left(\frac{A_r}{A_A}\right)^2 \left(1 - \frac{w_L}{w_T}\right)^2} \quad (B12)$$

The annulus wall friction term  $\frac{P_1 - P_A}{q_r}$  of equation (3) can be found from

$$\frac{P_1 - P_A}{q_r} = \int_0^{x/L} \left(\frac{f_{AL}}{r_A}\right) \left(\frac{q_A}{q_r}\right) d\left(\frac{x}{L}\right) \quad (B13)$$

which is equal to

$$\frac{P_1 - P_A}{q_r} = \frac{2f}{\tan \alpha} \int_0^{x/L} \frac{\left(\frac{q_A}{q_r}\right)}{\left(1 - \frac{x}{L}\right)} d\left(\frac{x}{L}\right) \quad (B14)$$

for a given value of  $\alpha$  and assuming a constant value of  $f = 0.005$ .

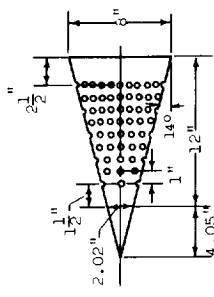
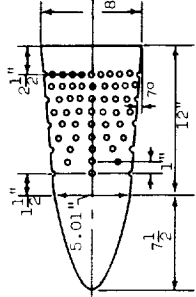
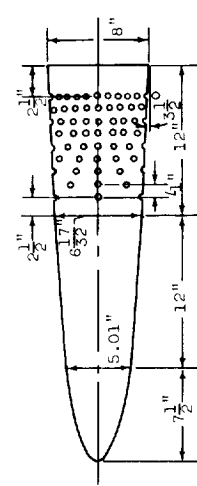
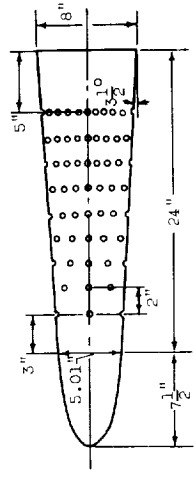
## REFERENCES

1. Graves, Charles C., and Grobman, Jack S.: Theoretical Analysis of Total-Pressure Loss and Airflow Distribution for Tubular Turbojet Combustors with Constant Annulus and Liner Cross-Sectional Areas. NACA RM E56IO4, 1957.
2. Dittrich, Ralph T., and Graves, Charles C.: Discharge Coefficients for Combustor-Liner Air-Entry Holes. I - Circular Holes with Parallel Flow. NACA TN 3663, 1956.
3. Dittrich, Ralph T.: Discharge Coefficients for Combustor-Liner Air-Entry Holes. II - Flush Rectangular Holes, Step Louvers, and Scoops. NACA TN 3924, 1958.

E-126

CQ-3

TABLE I. - DIMENSIONS OF LINER MODELS

Model	Configuration	Combustor length, $L$ , in.	Ratio of combustor length to reference diameter, $L/D$	Liner-wall inclination angle, $\alpha$ , deg	Blocked area at station 2, $A_{L,2}/A_T$	Number of holes (a)	Ratio of liner total open hole area to reference area, $A_h, \eta/A_T$	
							1/2-In. hole	5/8-In. 3/4-In. hole
A		12	$1\frac{1}{2}$	14	0.06	108	0.422	0.659
B		12	$1\frac{1}{2}$	7	0.40	108	0.422	0.659
C		12	$1\frac{1}{2}$	$3\frac{1}{2}$	0.67	108	0.422	0.659
D		24	3	$3\frac{1}{2}$	0.40	108	0.422	0.659

<sup>a</sup>Holes were spaced symmetrically around liner with number of holes per row as follows: 4, 6, 8, 10, 12, 14, 16, 18, and 20.

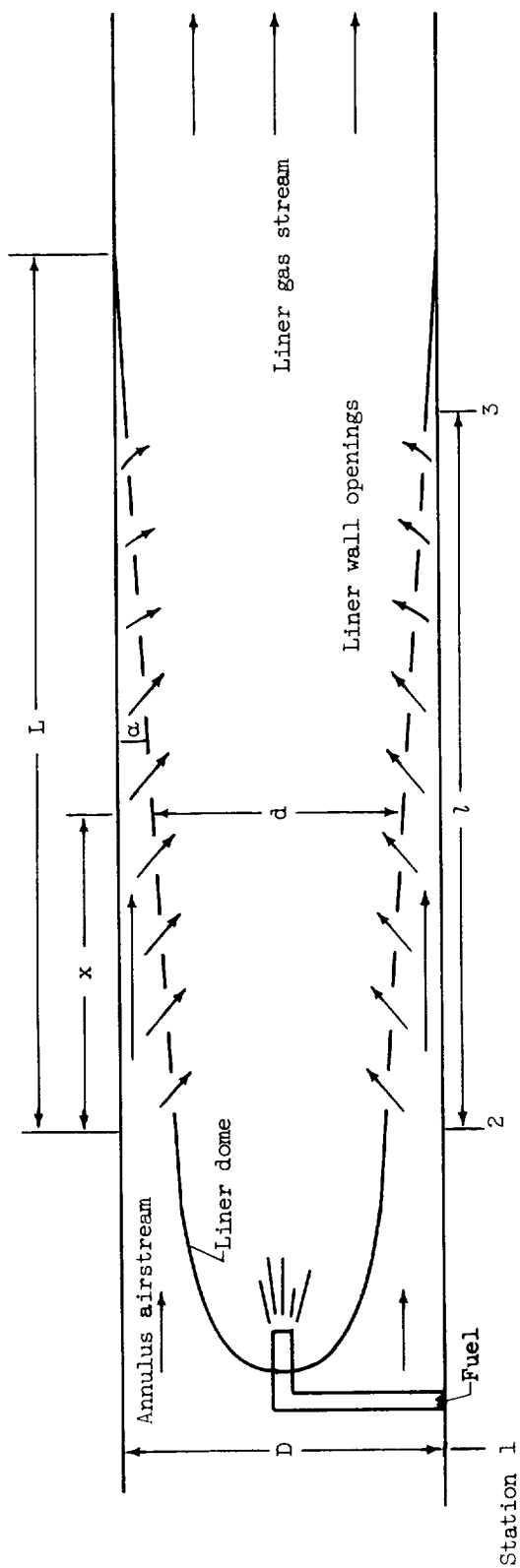


Figure 1. - Schematic diagram of tubular combustor with tapered liner.

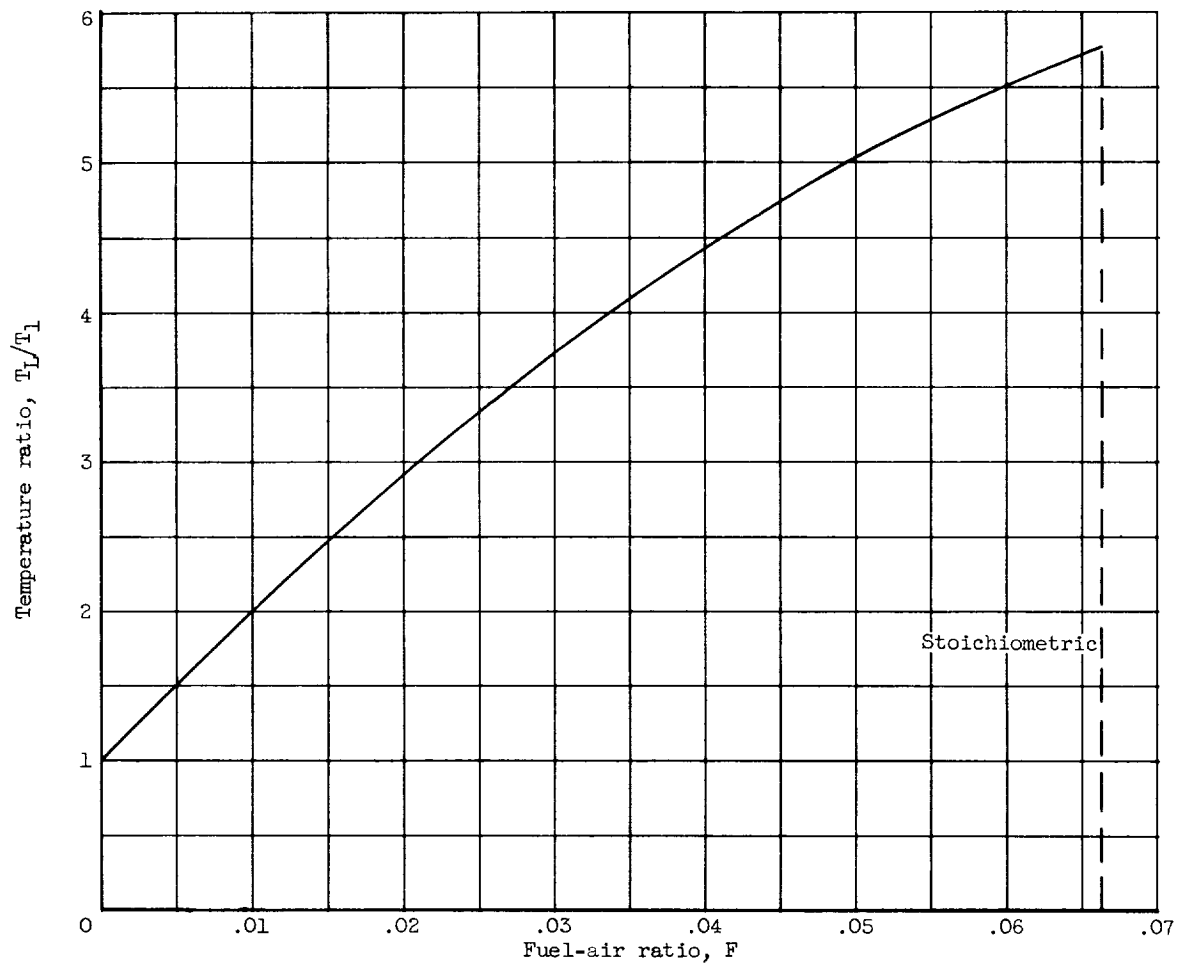


Figure 2. - Variation of exhaust to inlet temperature ratio with fuel-air ratio for combustion of normal-octane fuel with 100 percent efficiency. Initial air temperature  $728^{\circ}\text{R}$ ; initial fuel temperature  $540^{\circ}\text{R}$ ; pressure, 1 atmosphere (ref. 1).

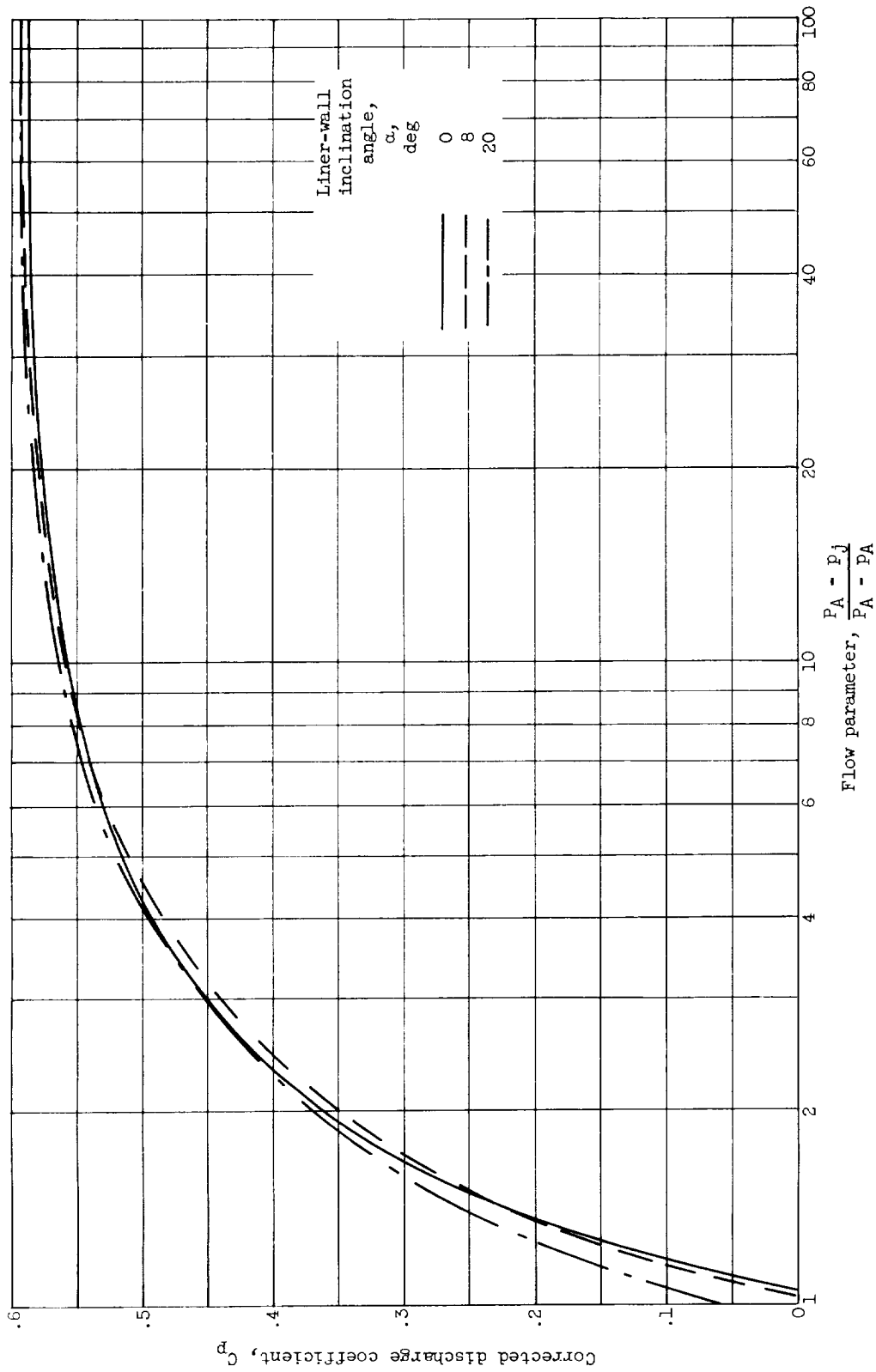


Figure 3. - Variation of corrected discharge coefficient with flow parameter for various liner-wall inclinations. Flush circular holes with 0.75-inch diameter; 0.040-inch wall thickness (ref. 3).

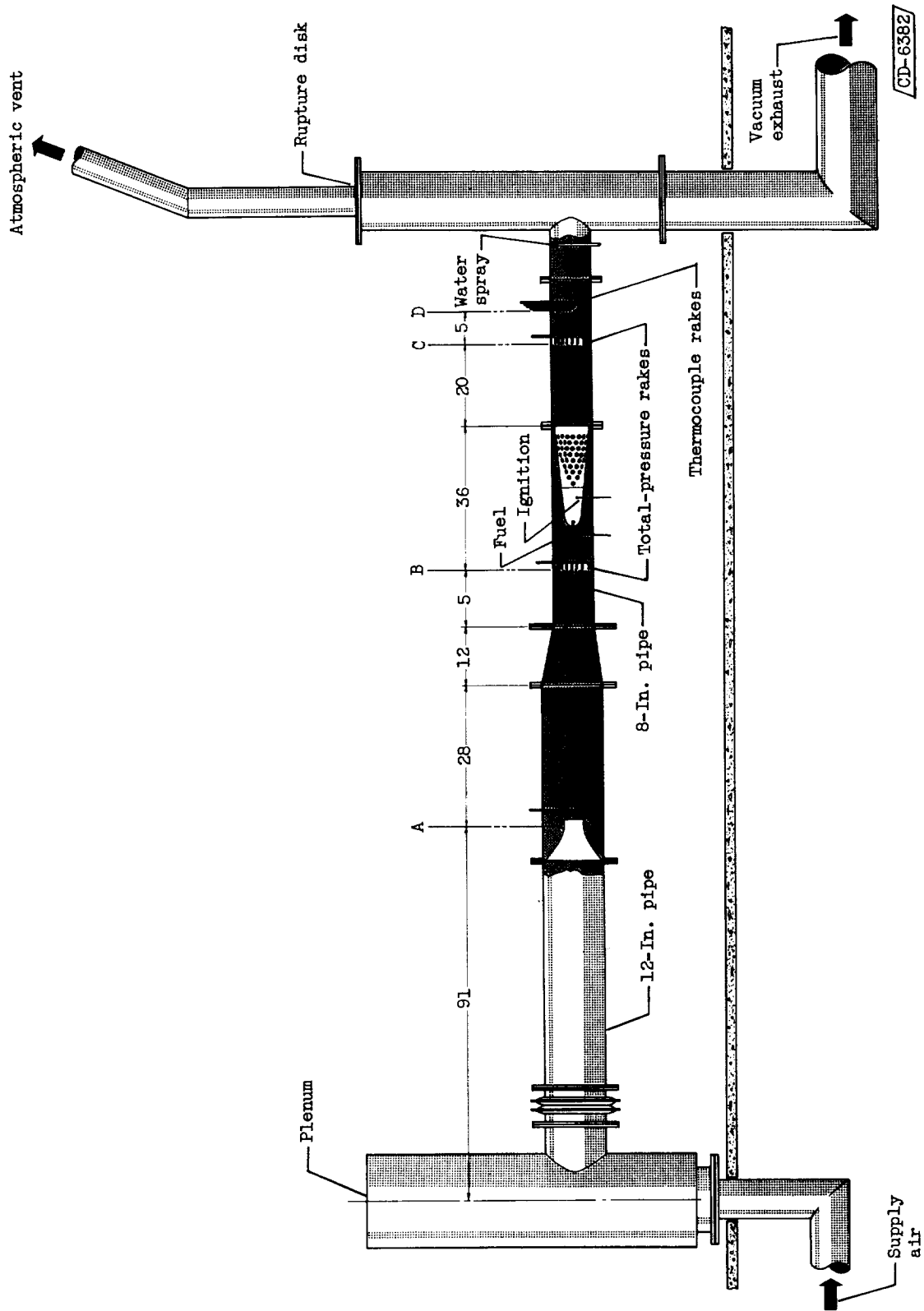


Figure 4. - Schematic diagram of research combustor installation. (All dimensions in inches.)



E-126

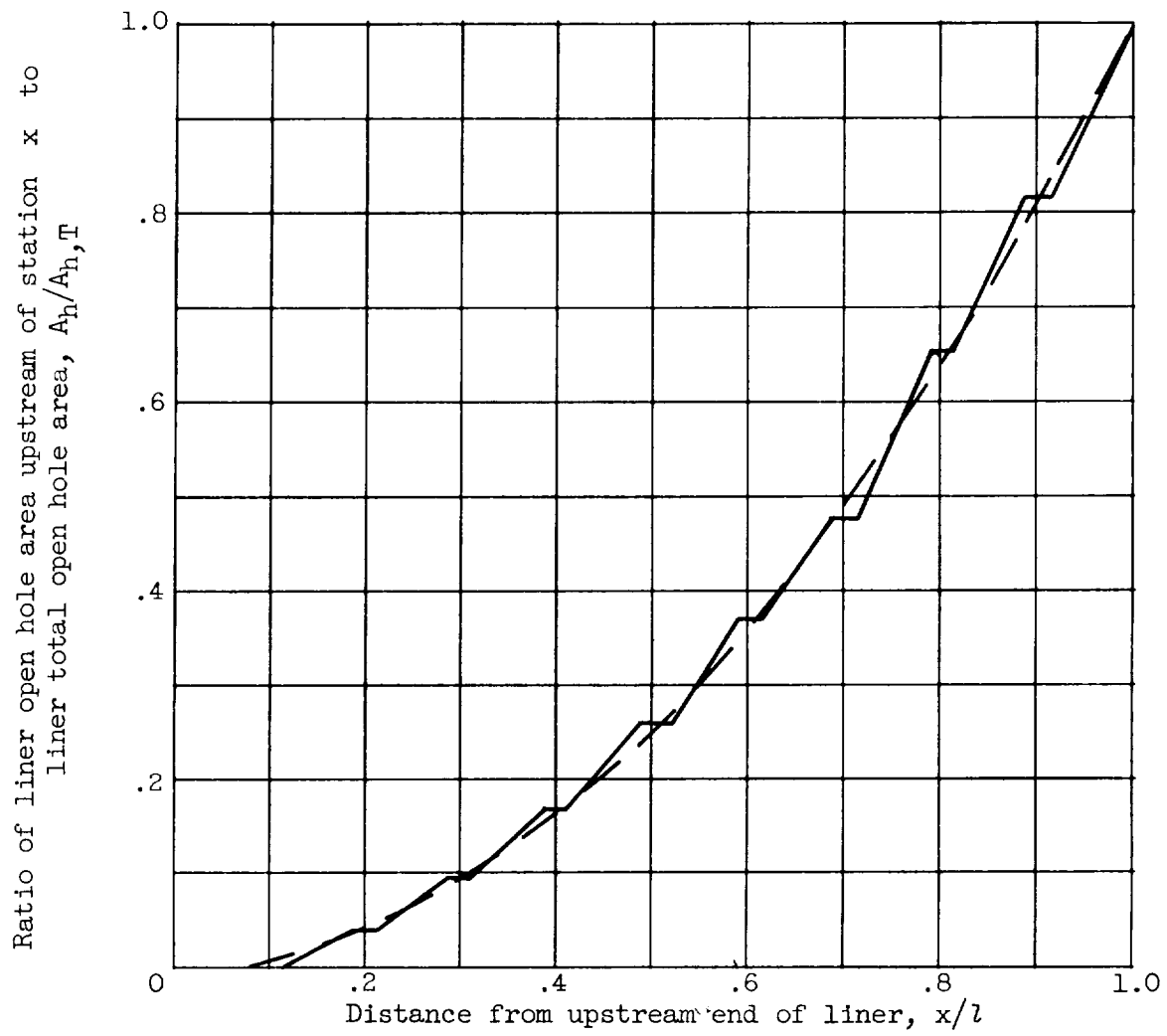


Figure 5. - Axial liner hole area distribution of experimental liners.

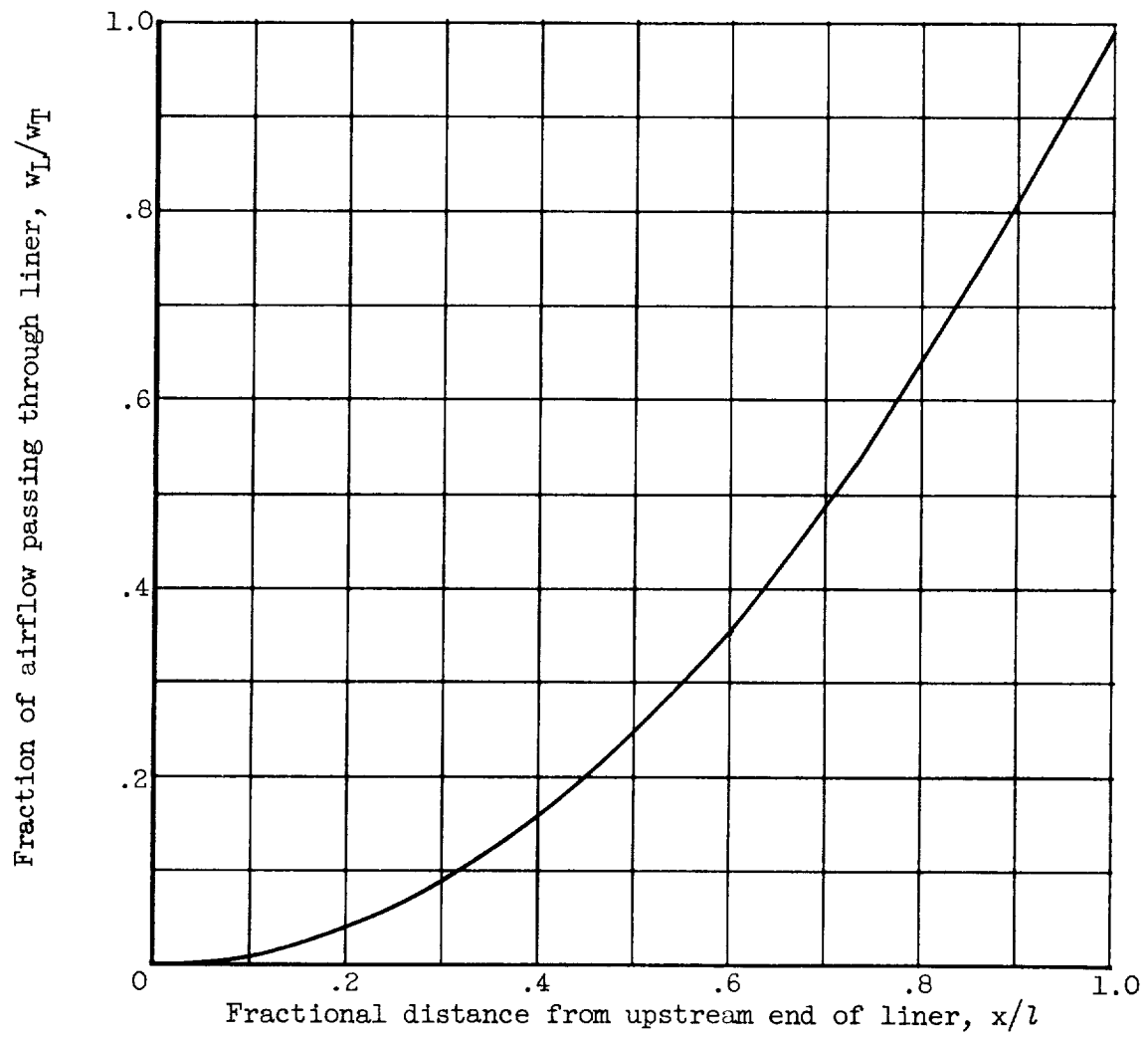


Figure 6. - Axial airflow distribution assumed in calculations.

E-126

CQ-4

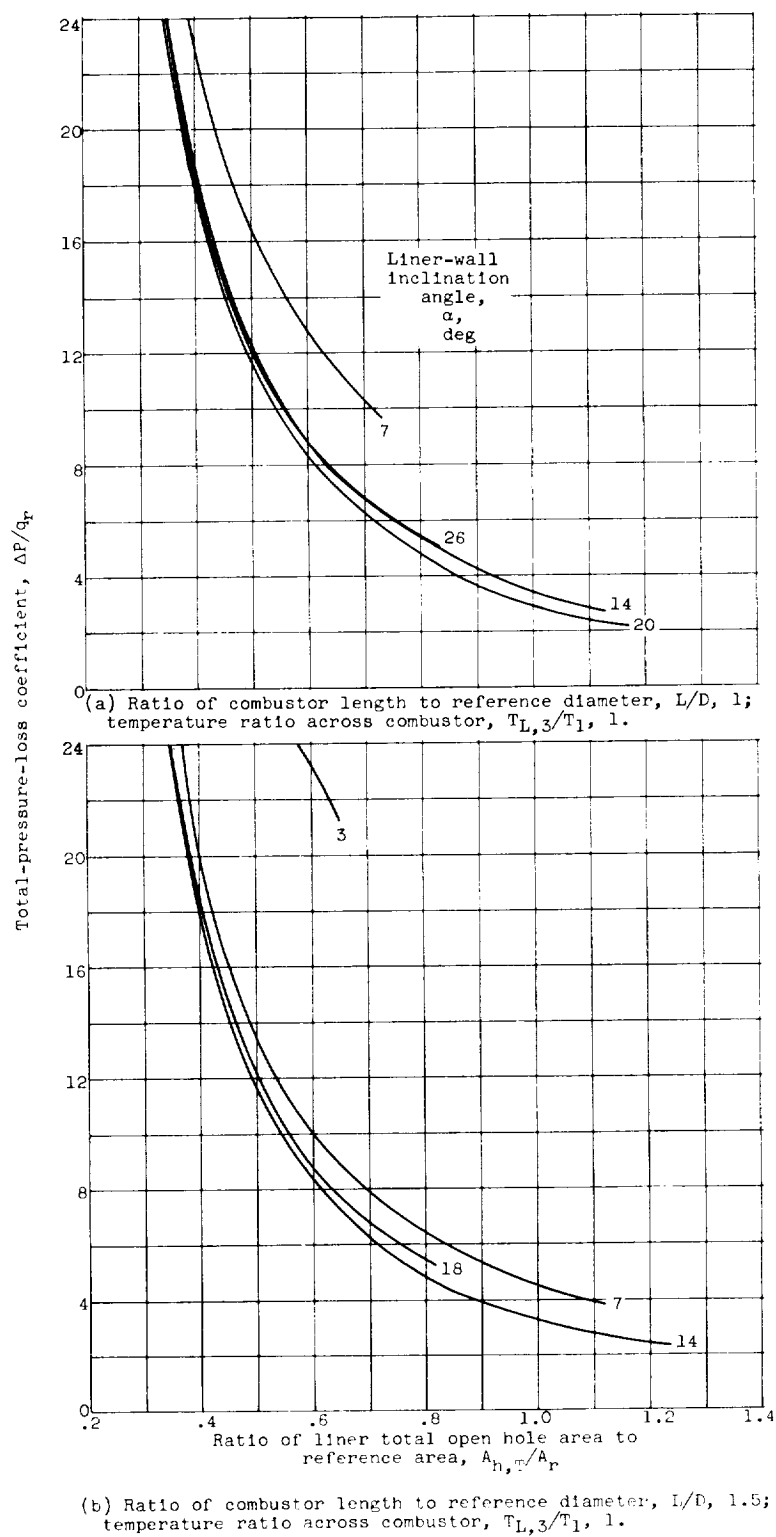


Figure 7. - Variation of calculated total-pressure-loss coefficient with area ratio for various wall inclinations.

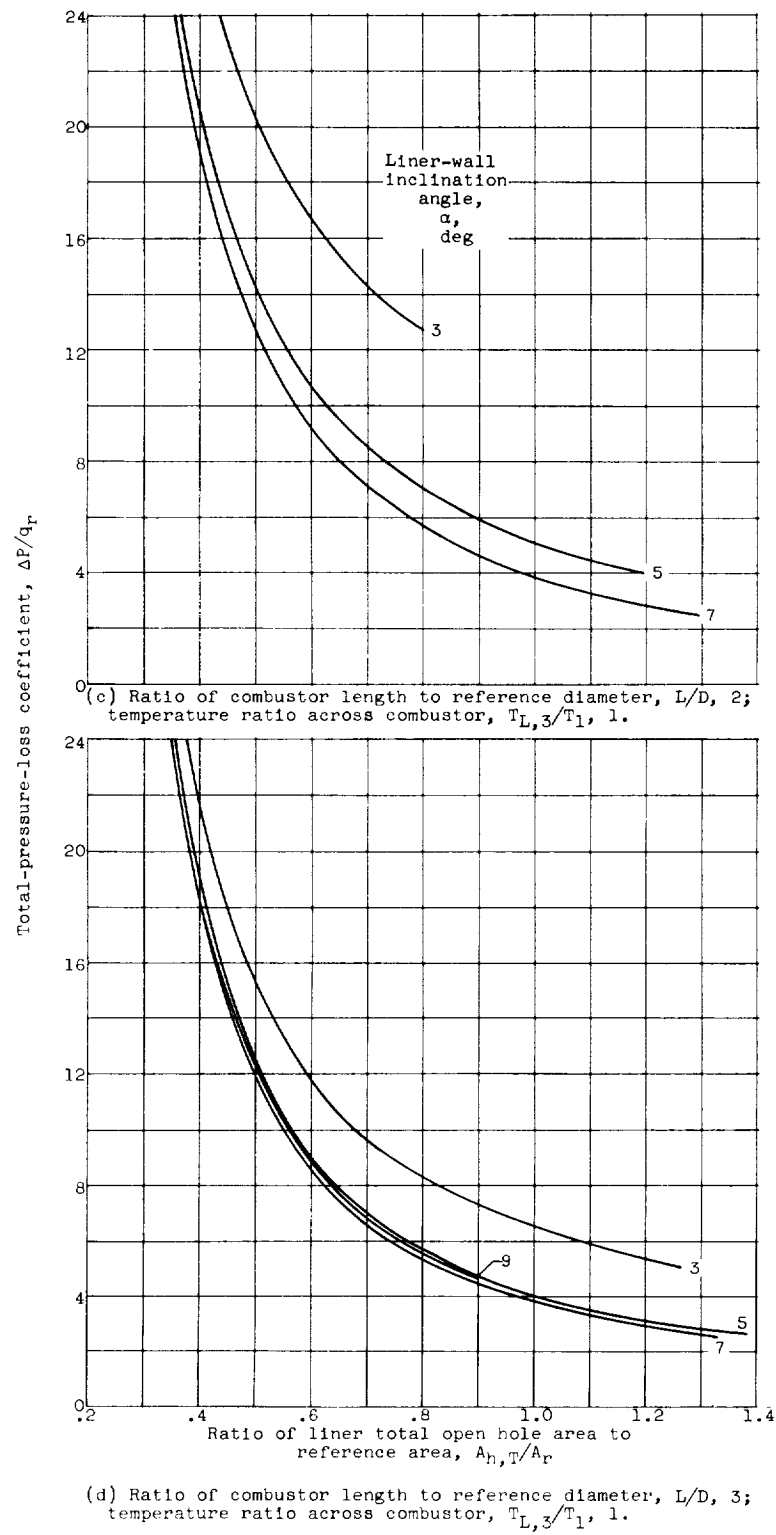
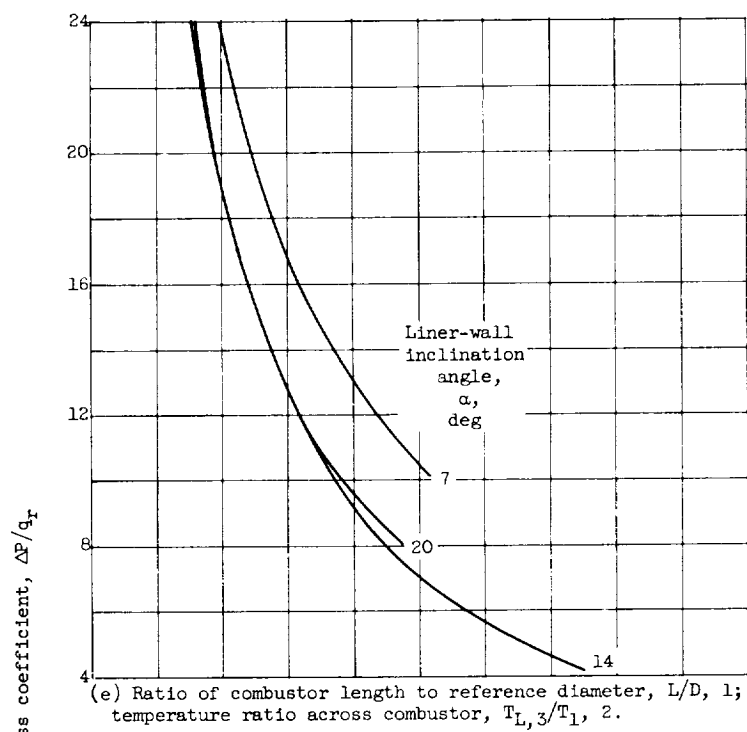


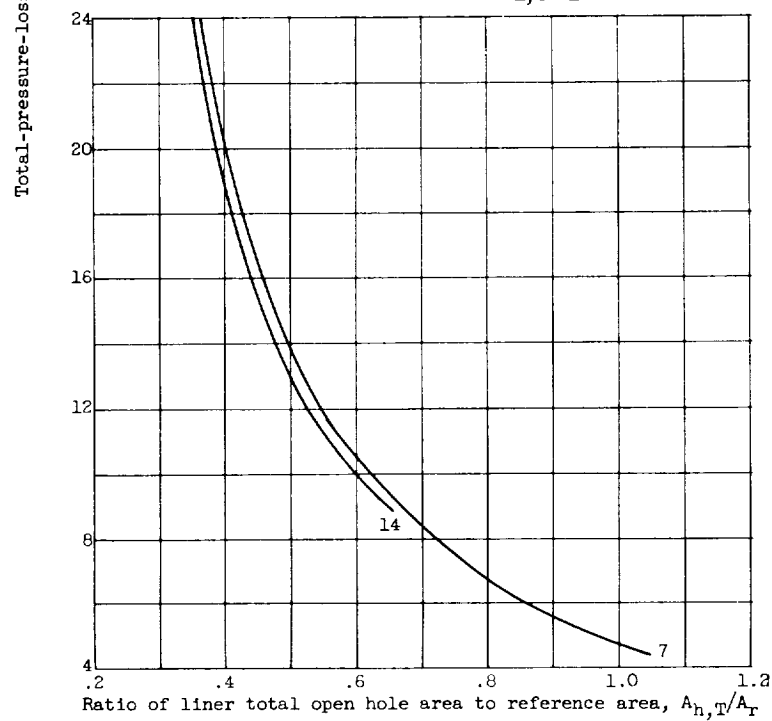
Figure 7. - Continued. Variation of calculated total-pressure-loss coefficient with area ratio for various wall inclinations.

E-126

CQ-4 back

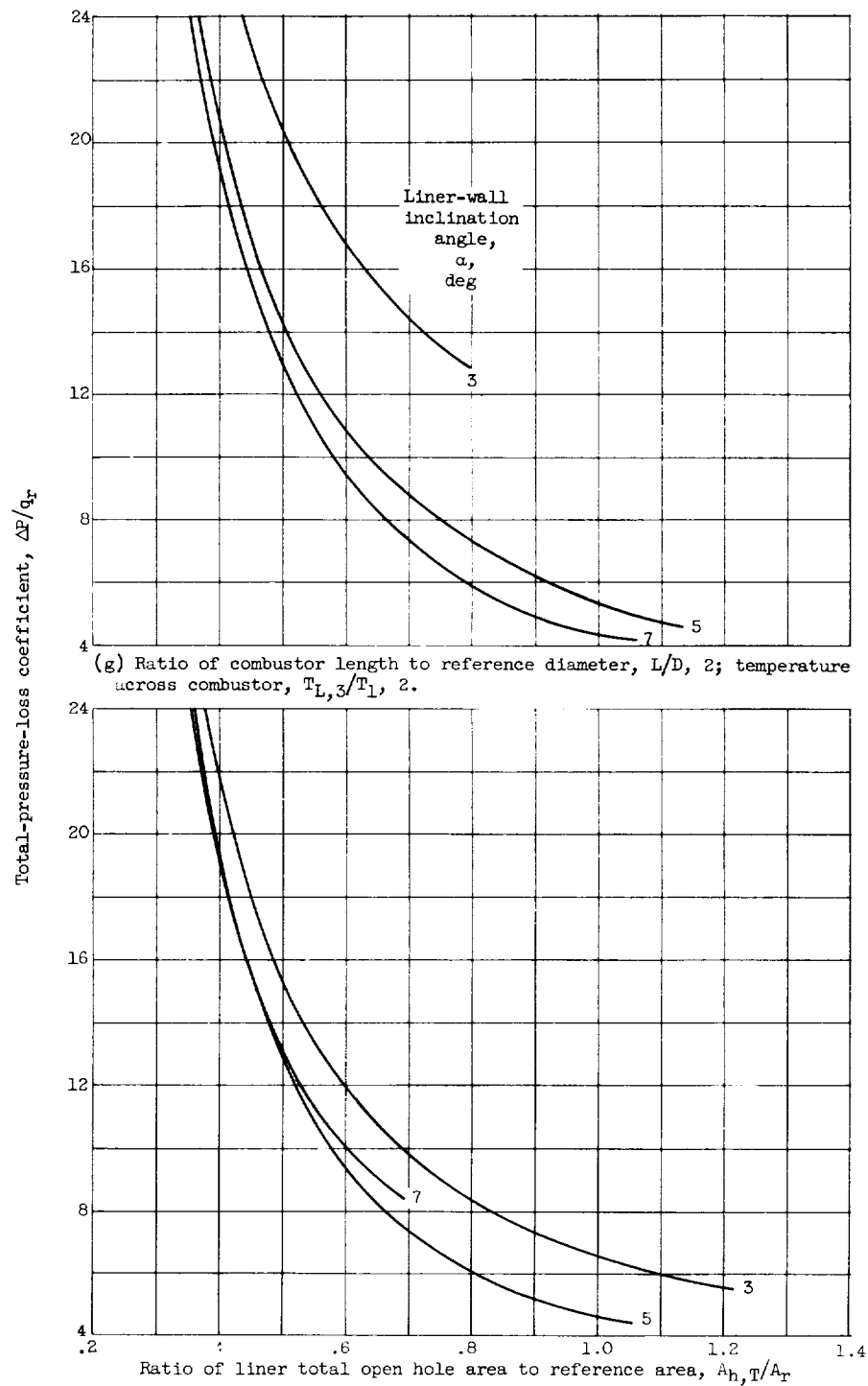


(e) Ratio of combustor length to reference diameter,  $L/D$ , 1; temperature ratio across combustor,  $T_{L,3}/T_1$ , 2.



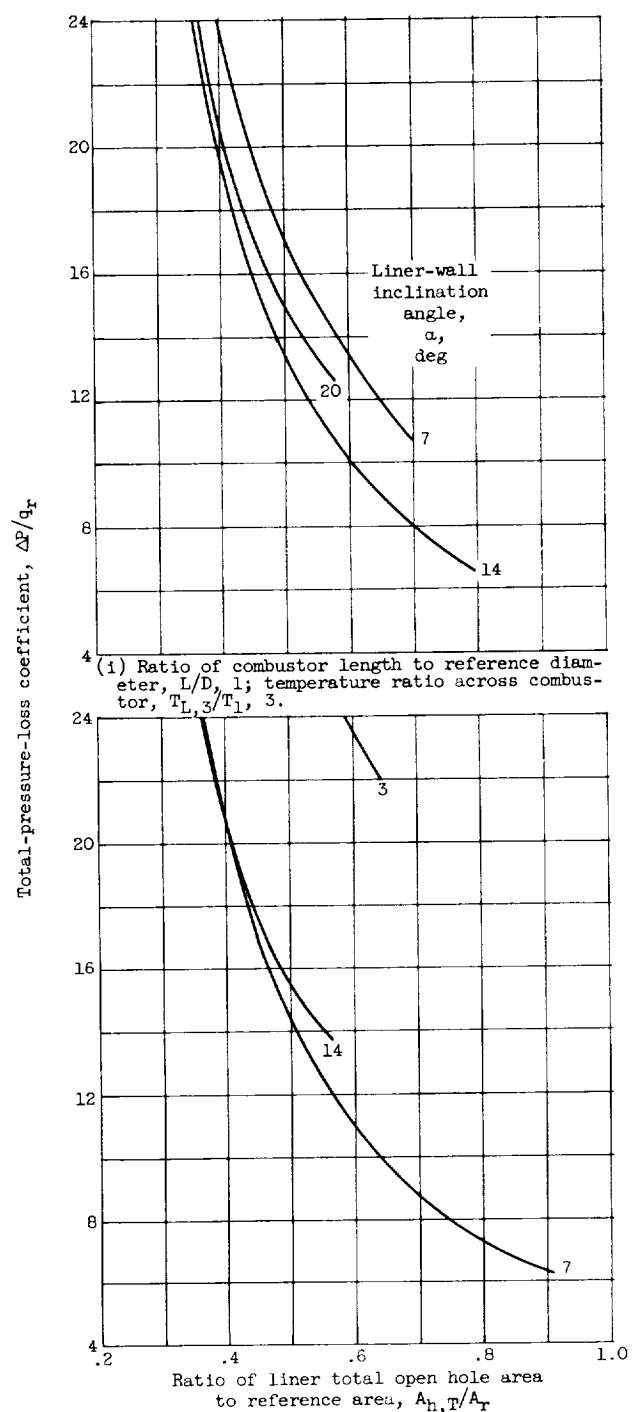
(f) Ratio of combustor length to reference diameter,  $L/D$ , 1.5; temperature ratio across combustor,  $T_{L,3}/T_1$ , 2.

Figure 7. - Continued. Variation of calculated total-pressure-loss coefficient with area ratio for various wall inclinations.



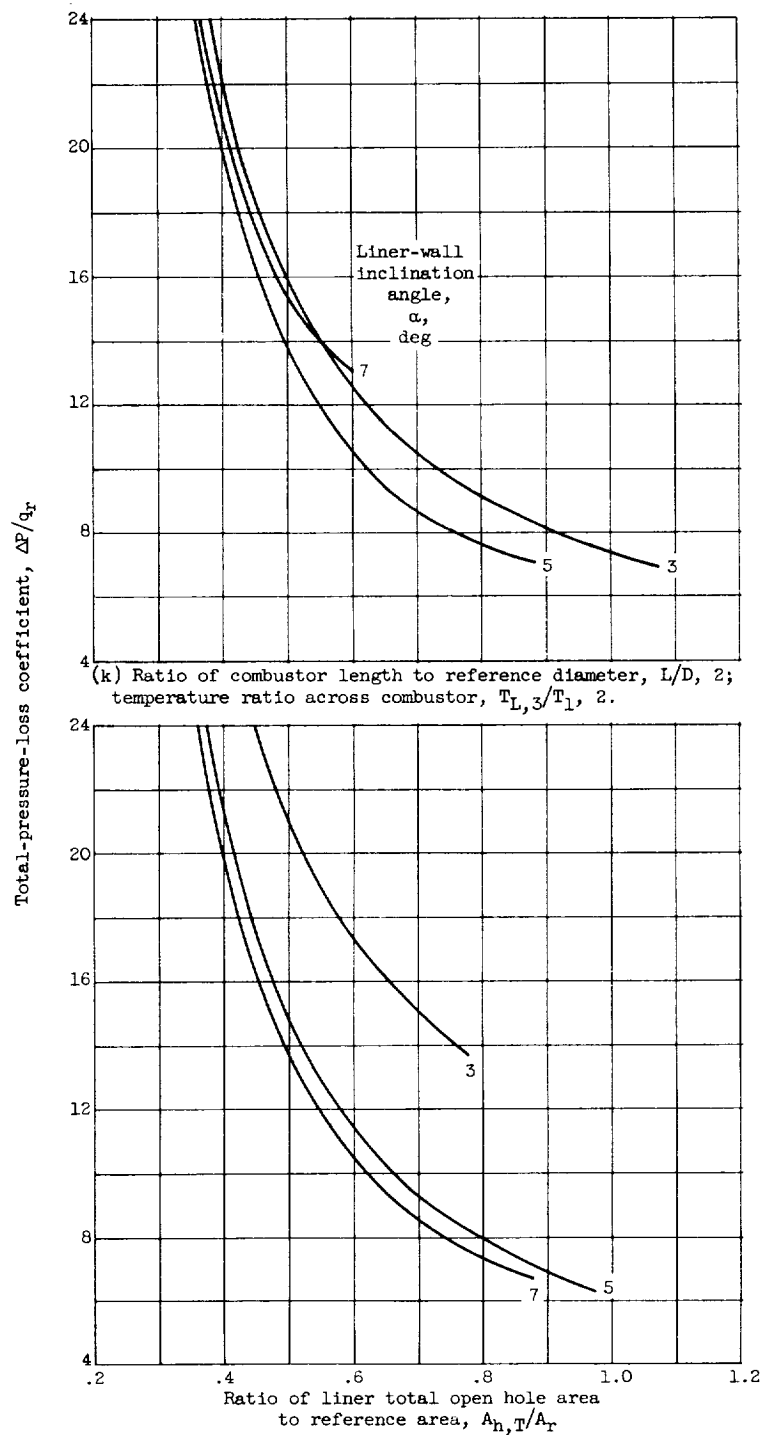
(h) Ratio of combustor length to reference diameter,  $L/D$ , 3; temperature ratio across combustor,  $T_{L,3}/T_1$ , 2.

Figure 7. - Continued. Variation of calculated total-pressure-loss coefficient with area ratio for various wall inclinations.



(j) Ratio of combustor length to reference diameter,  $L/D_r$ , 1.5; temperature ratio across combustor,  $T_{L,3}/T_1$ , 3.

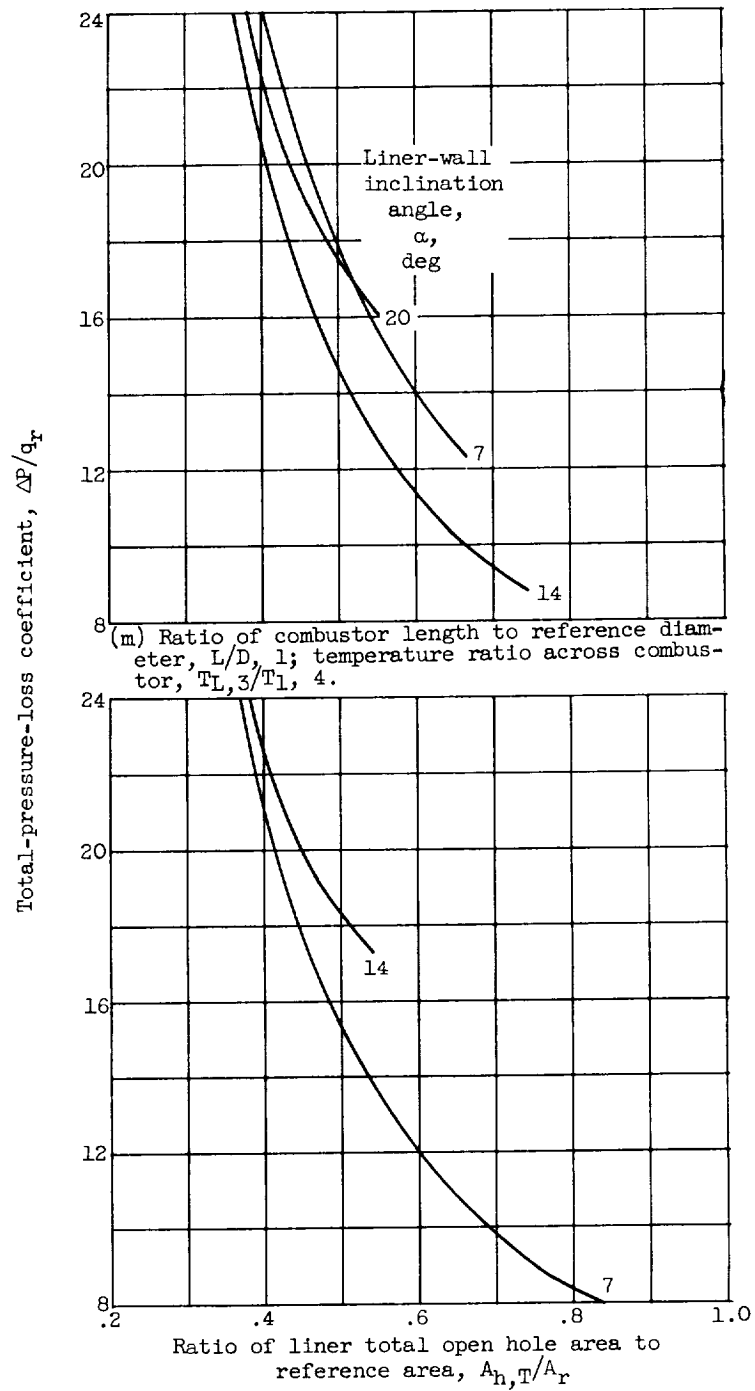
Figure 7. - Continued. Variation of calculated total-pressure-loss coefficient with area ratio for various wall inclinations.



(l) Ratio of combustor length to reference diameter,  $L/D$ , 3; temperature ratio across combustor,  $T_{L,3}/T_1$ , 3.

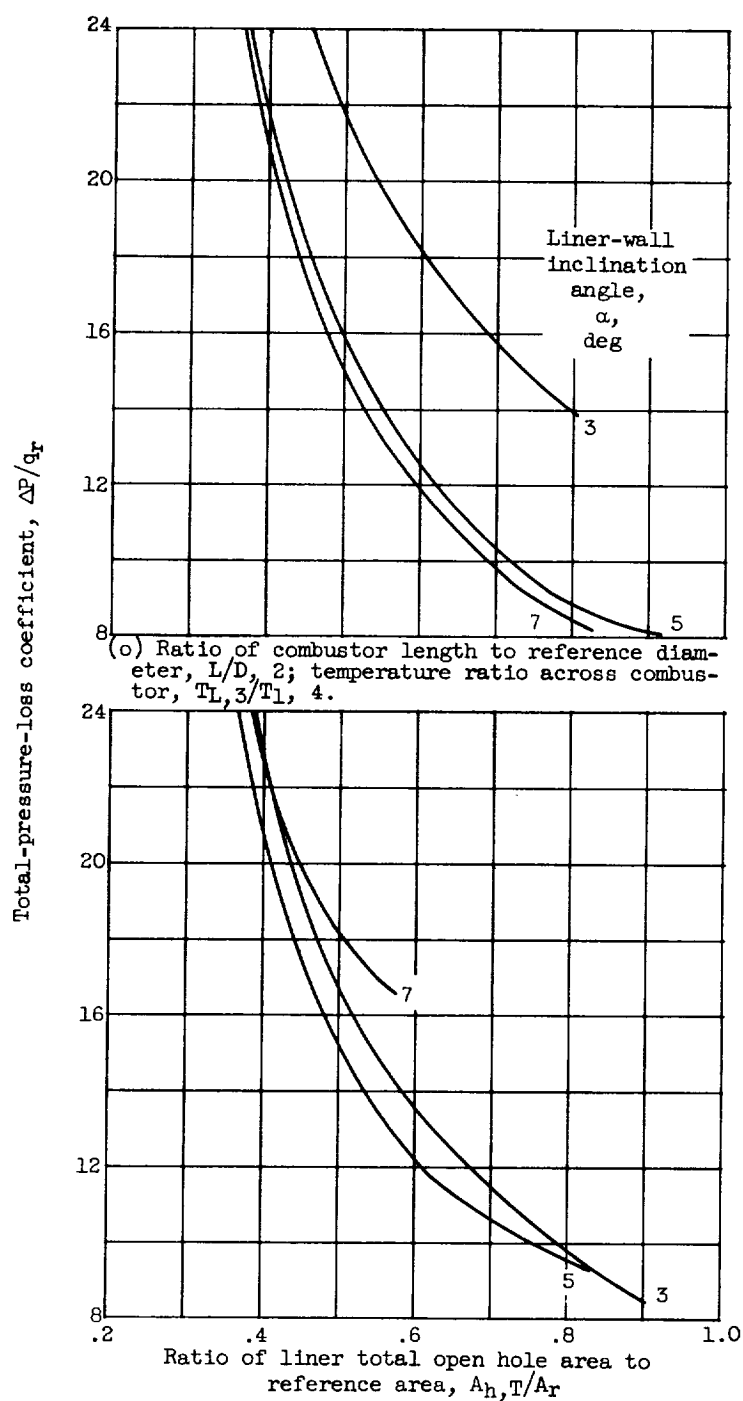
Figure 7. - Continued. Variation of calculated total-pressure-loss coefficient with area ratio for various wall inclinations.





(n) Ratio of combustor length to reference diameter,  $L/D$ , 1.5; temperature ratio across combustor,  $T_{L,3}/T_1$ , 4.

Figure 7. - Continued. Variation of calculated total-pressure-loss coefficient with area ratio for various wall inclinations.



(p) Ratio of combustor length to reference diameter,  $L/D$ , 3; temperature-ratio across combustor,  $T_{L,3}/T_1$ , 4.

Figure 7. - Concluded. Variation of calculated total-pressure-loss coefficient with area ratio for various wall inclinations.

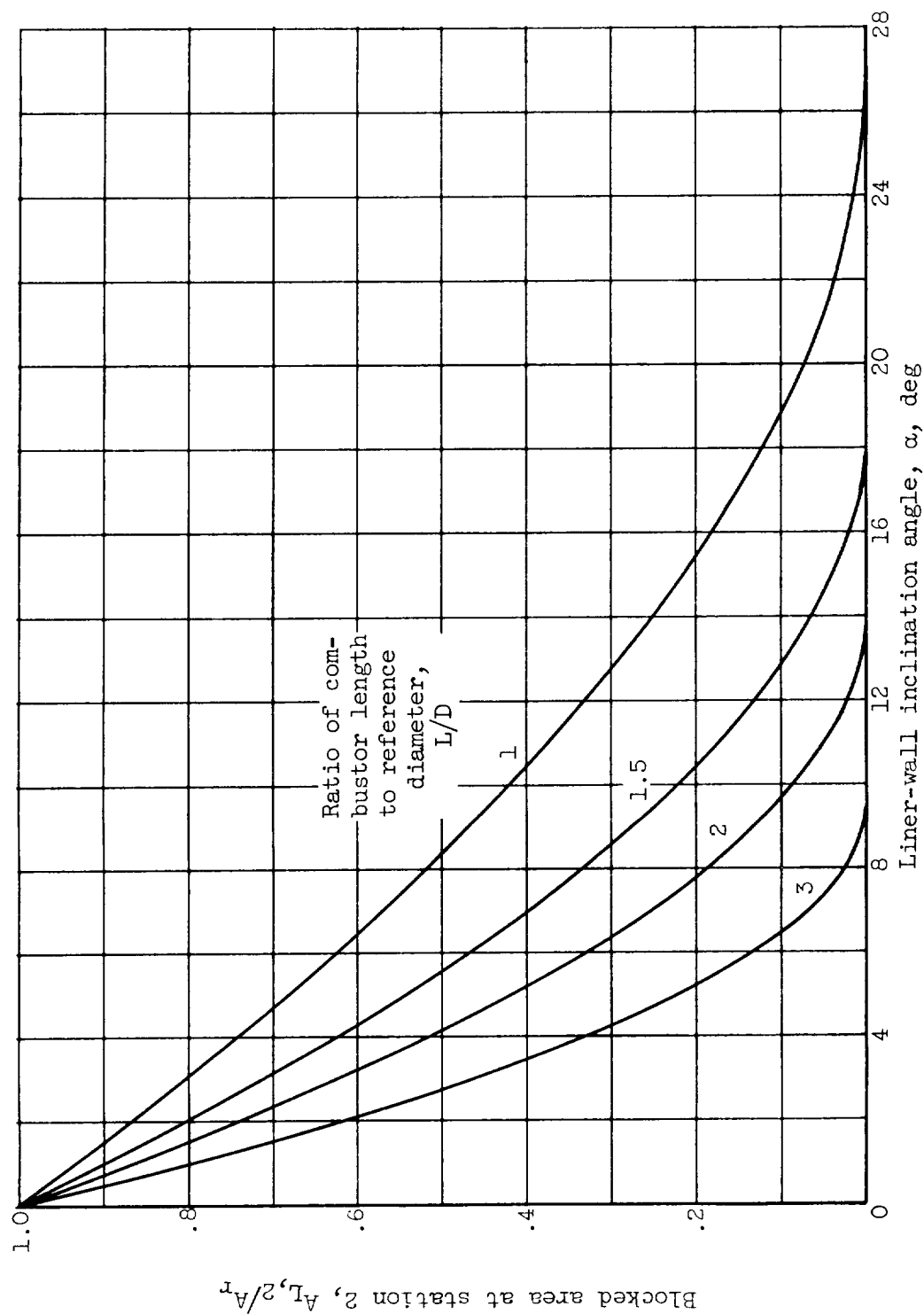


Figure 8. - Variation of combustor blocked area at station 2 (fig. 2) with liner-wall inclination for various values of  $L/D$ .

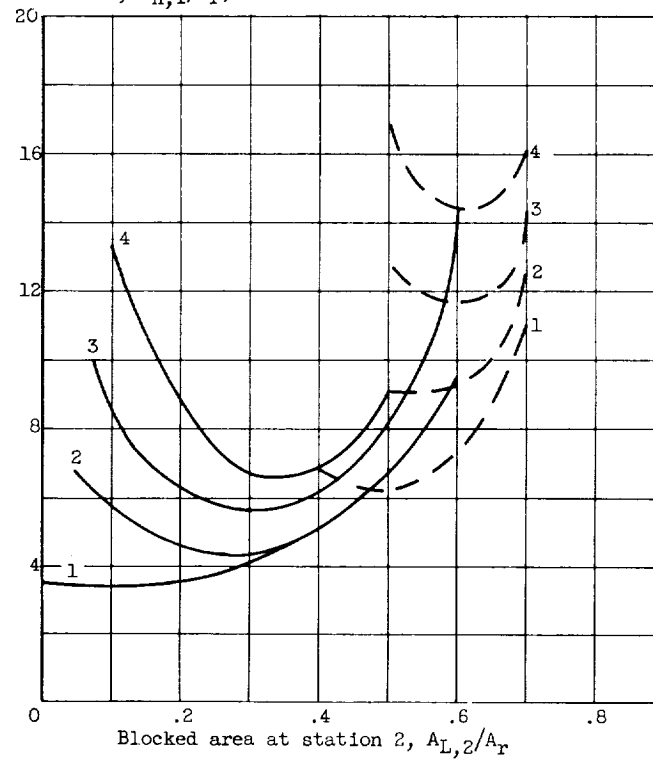
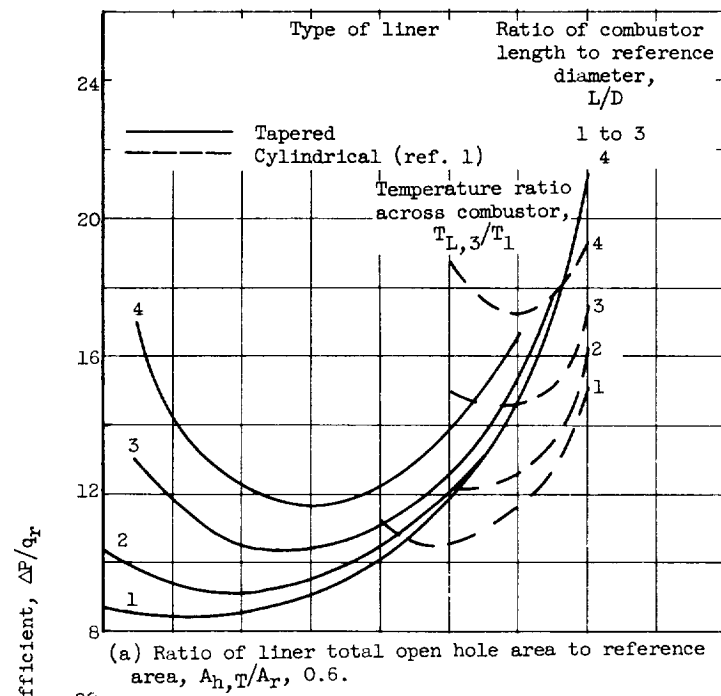


Figure 9. - Variation of total-pressure loss coefficient with blocked area at station 2 for various temperature ratios.

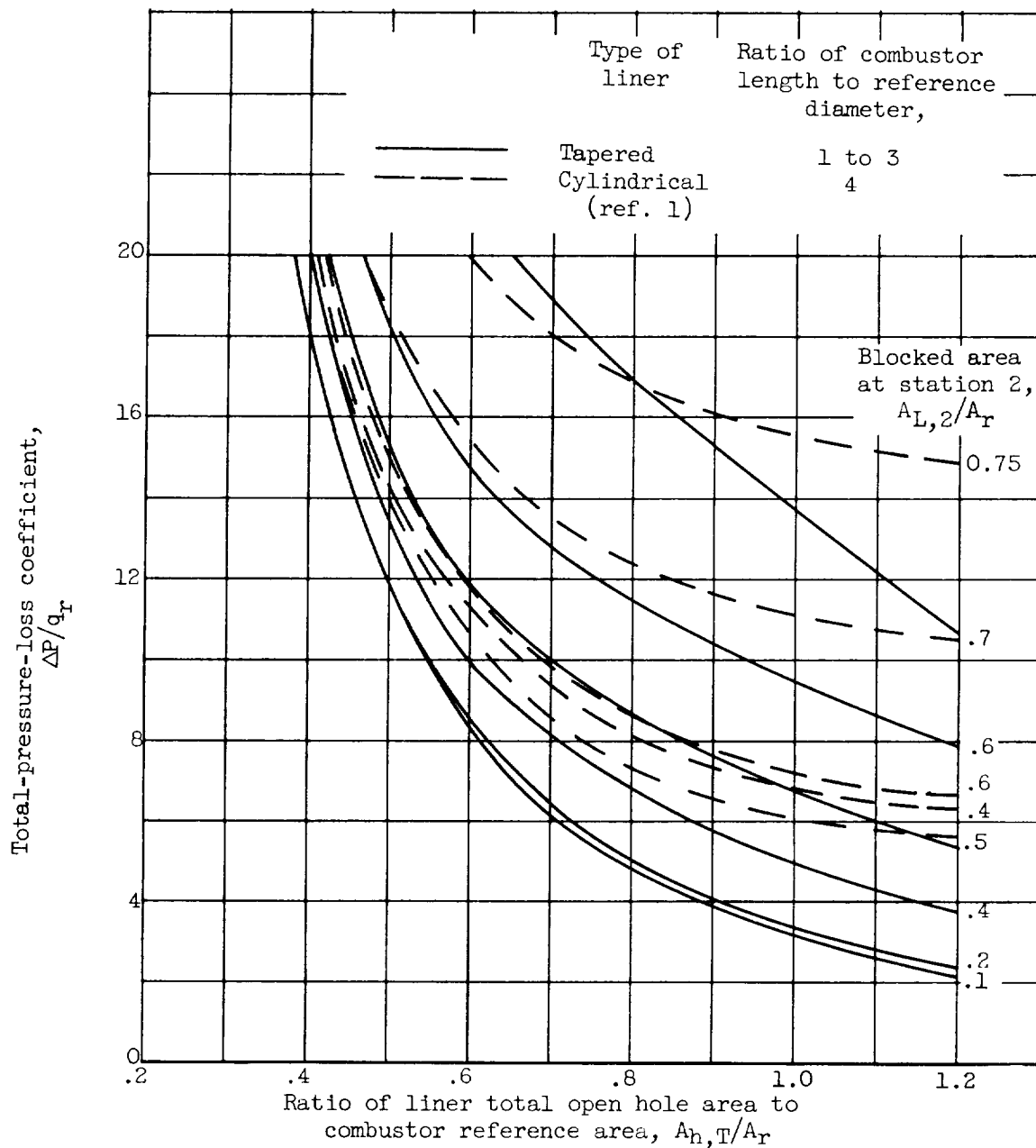
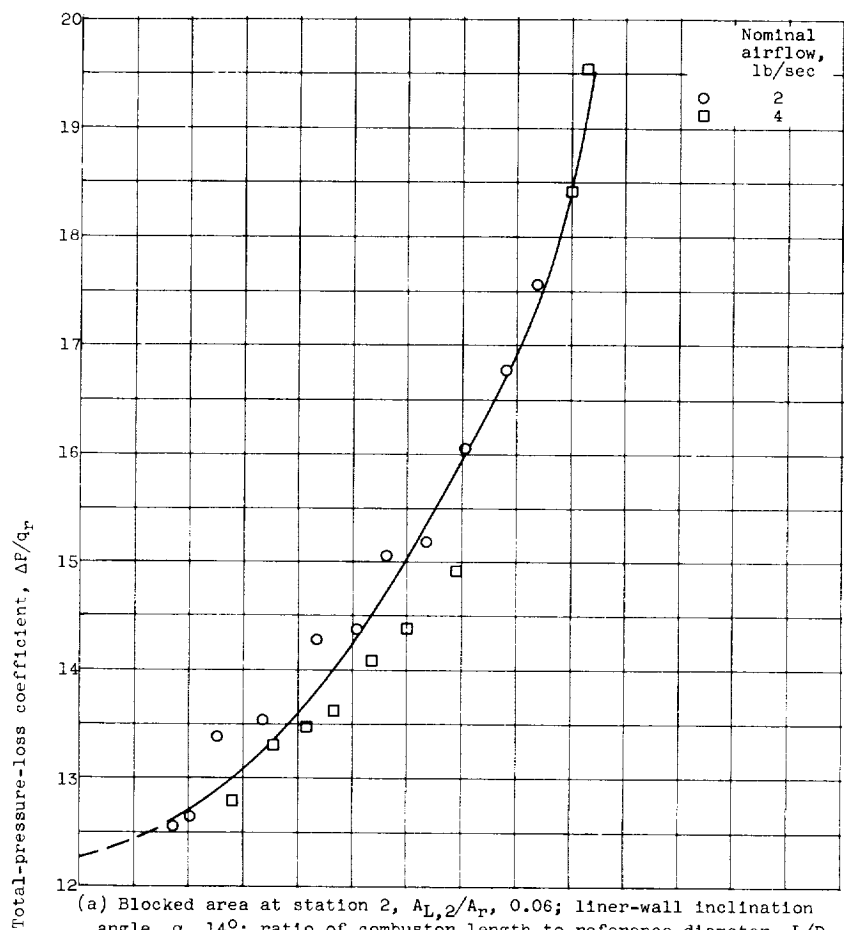
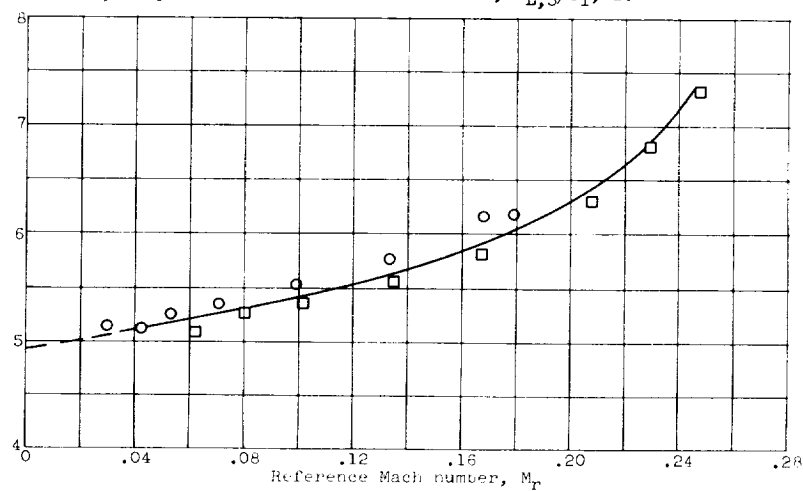


Figure 10. , Variation of calculated total-pressure-loss coefficient with ratio of liner total open hole area to combustor reference area for various values of blocked area at station 2.

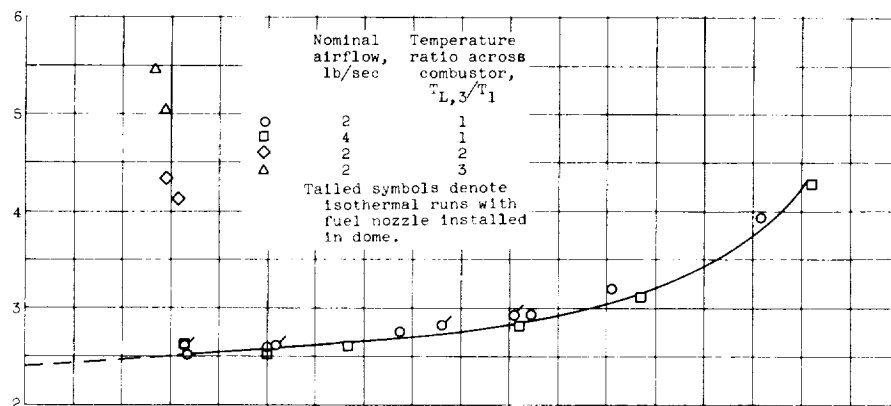


(a) Blocked area at station 2,  $A_{L,2}/A_r$ , 0.06; liner-wall inclination angle,  $\alpha$ ,  $14^\circ$ ; ratio of combustor length to reference diameter,  $L/D$ , 1.5; ratio of liner total open hole area to reference area,  $A_{h,T}/A_r$ , 0.422; temperature ratio across combustor,  $T_{L,3}/T_1$ , 1.

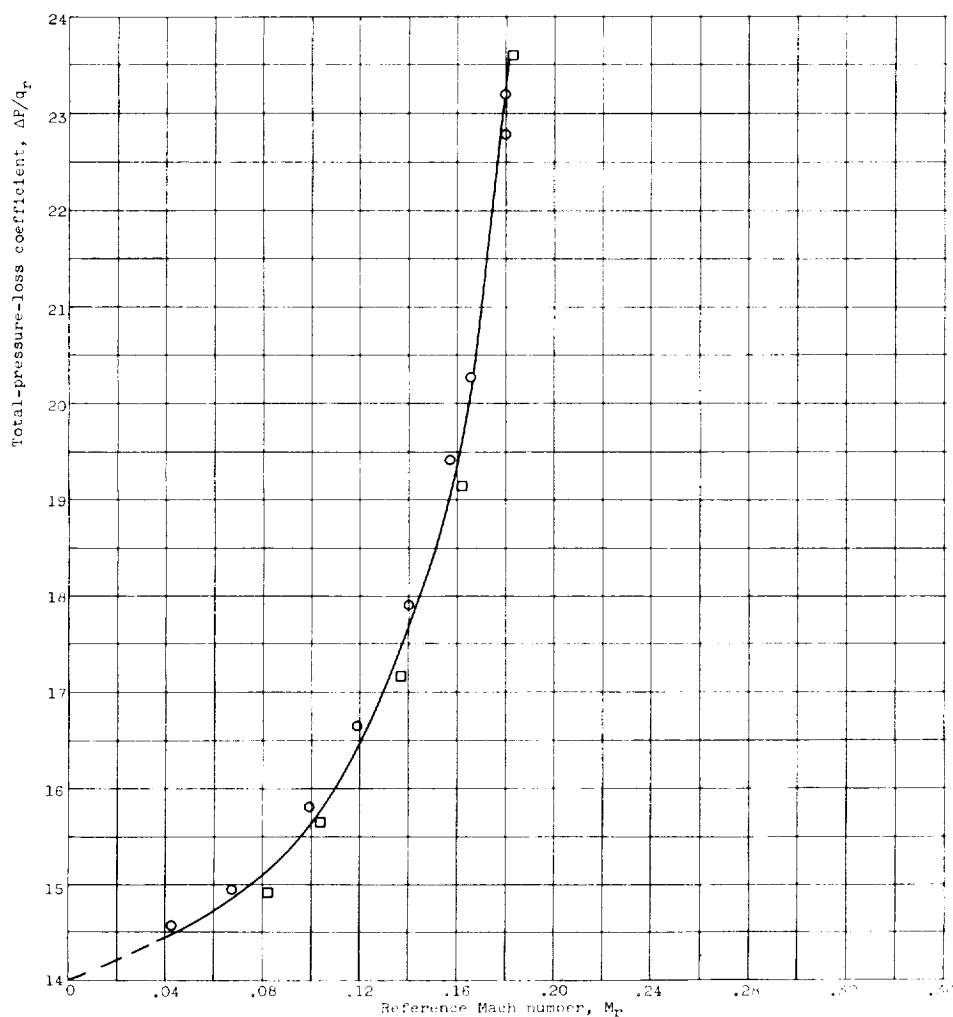


(b) Blocked area at station 2,  $A_{L,2}/A_r$ , 0.06; liner-wall inclination angle,  $\alpha$ ,  $14^\circ$ ; ratio of combustor length to reference diameter,  $L/D$ , 1.5; ratio of liner total open hole area to reference area,  $A_{h,T}/A_r$ , 0.659; temperature ratio across combustor,  $T_{L,3}/T_1$ , 1.

Figure 11. - Variation of experimental total-pressure-loss coefficient with reference Mach number for 12 tapered liners.

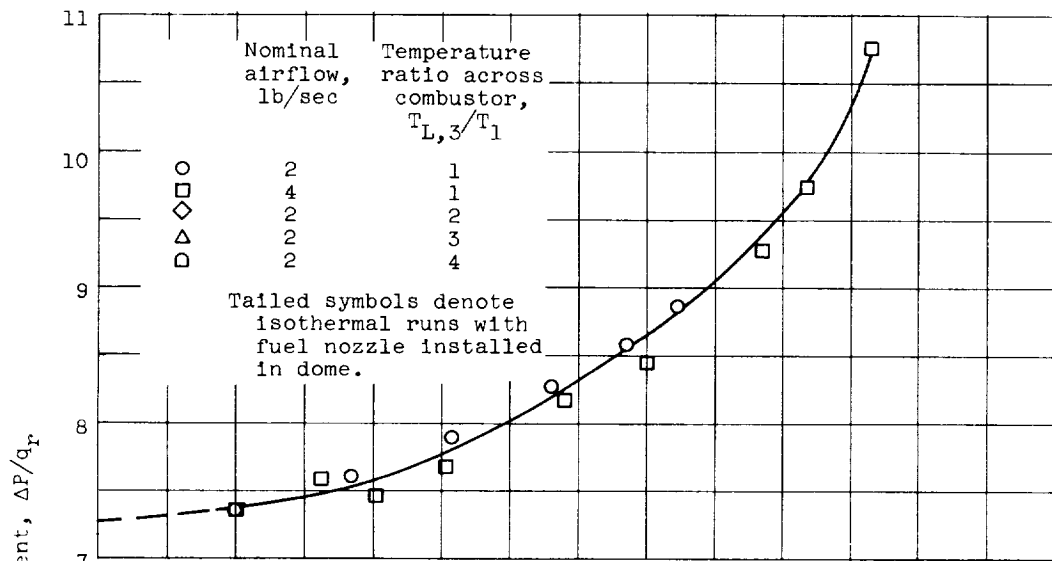


(c) Blocked area at station 2,  $A_{L,2}/A_P$ , 0.06; liner-wall inclination angle,  $\alpha$ ,  $14^\circ$ ; ratio of combustor length to reference diameter,  $L/D$ , 1.5; ratio of liner total open hole area to reference area,  $A_{h,T}/A_P$ , 0.95.

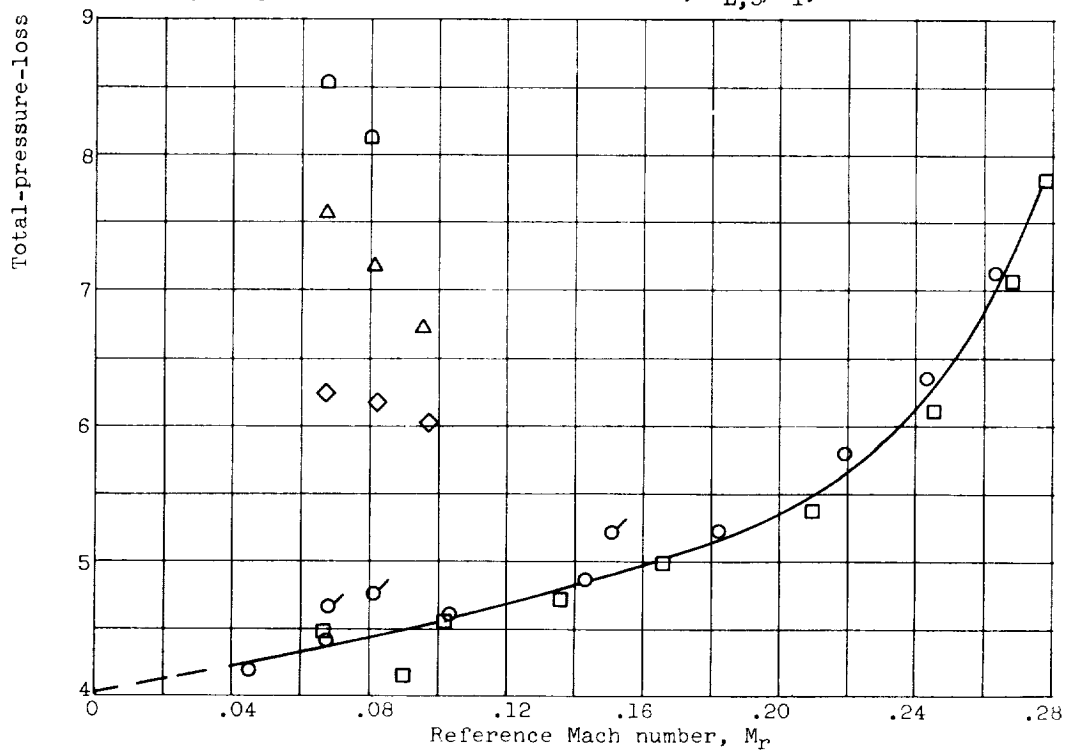


(d) Blocked area at station 2,  $A_{L,2}/A_P$ , 0.40; liner-wall inclination angle,  $\alpha$ ,  $7^\circ$ ; ratio of liner total open hole area to reference area,  $A_{h,T}/A_P$ , 0.422; temperature ratio across combustor,  $T_{L,3}/T_1$ , 1.

Figure 11. - Continued. Variation of experimental total-pressure-loss coefficient with reference Mach number for 12 tapered liners.



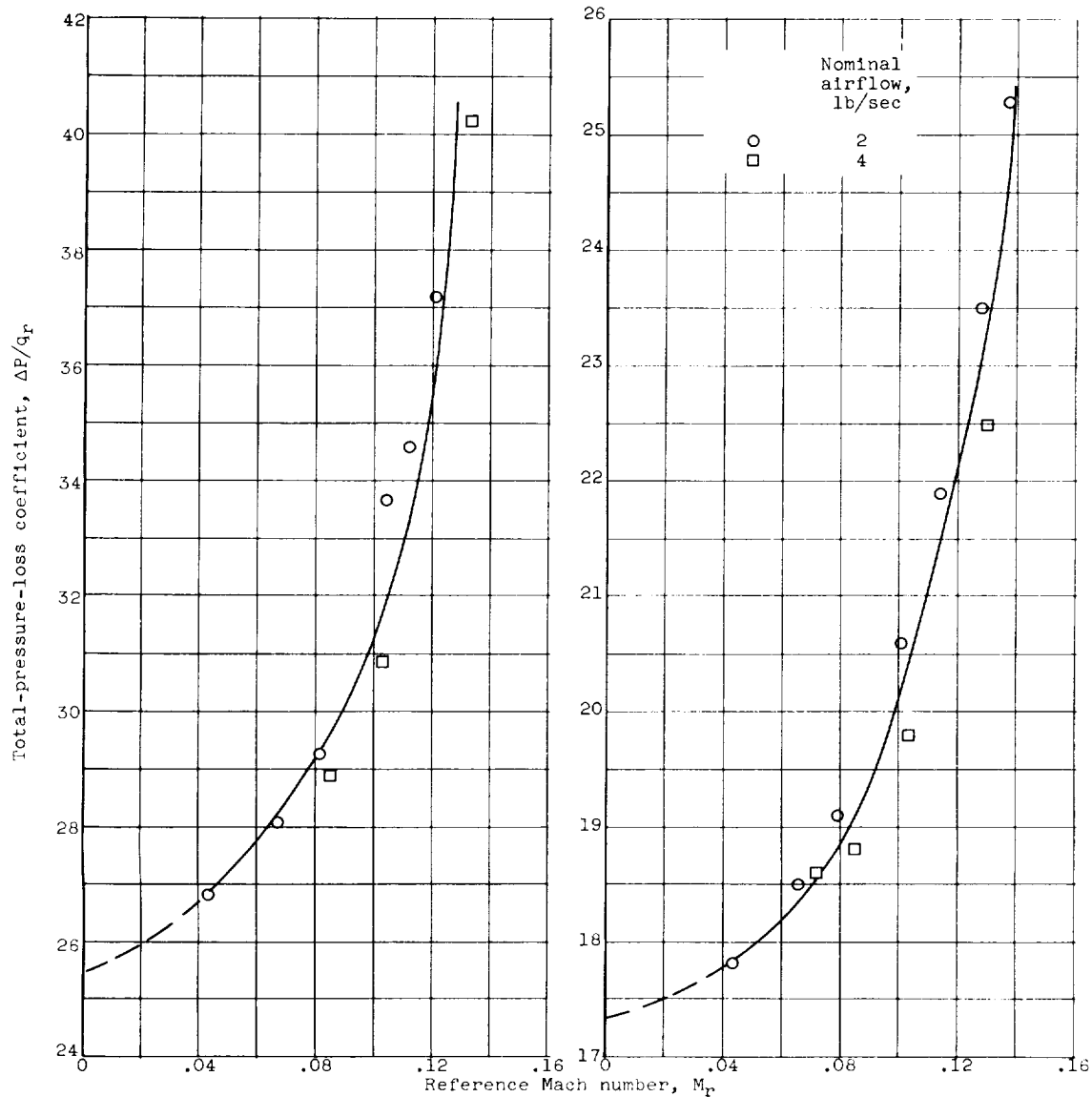
(e) Blocked area at station 2,  $A_{L,2}/A_r$ , 0.40; liner-wall inclination angle,  $\alpha$ ,  $70^\circ$ ; ratio of combustor length to reference diameter,  $L/D$ , 1.5; ratio of liner total open hole area to reference area,  $A_{h,T}/A_r$ , 0.659; temperature ratio across combustor,  $T_{L,3}/T_1$ , 1.



(f) Blocked area at station 2,  $A_{L,2}/A_4$ , 0.40; liner-wall inclination angle,  $\alpha$ ,  $70^\circ$ ; ratio of combustor length to reference diameter,  $L/D$ , 1.5; ratio of liner total open hole area to reference area,  $A_{h,T}/A_r$ , 0.950.

Figure 11. - Continued. Variation of experimental total-pressure-loss coefficient with reference Mach number for 12 tapered liners.





(g) Blocked area at station 2,  $A_{L,2}/A_r$ , 0.67; liner-wall inclination angle,  $\alpha$ ,  $310^\circ$ ; ratio of combustor length to reference diameter,  $L/D$ , 1.5; ratio of liner total open hole area to reference area,  $A_{h,T}/A_r$ , 0.422; temperature ratio across combustor  $T_{L,3}/T_1$ , 1.

(h) Blocked area at station 2,  $A_{L,2}/A_r$ , 0.67; liner-wall inclination angle,  $\alpha$ ,  $310^\circ$ ; ratio of combustor length to reference diameter,  $L/D$ , 1.5; ratio of liner total open hole area to reference area,  $A_{h,T}/A_r$ , 0.659; temperature ratio across combustor,  $T_{L,3}/T_1$ , 1.

Figure 11. - Continued. Variation of experimental total-pressure-loss coefficient with reference Mach number for 12 tapered liners.

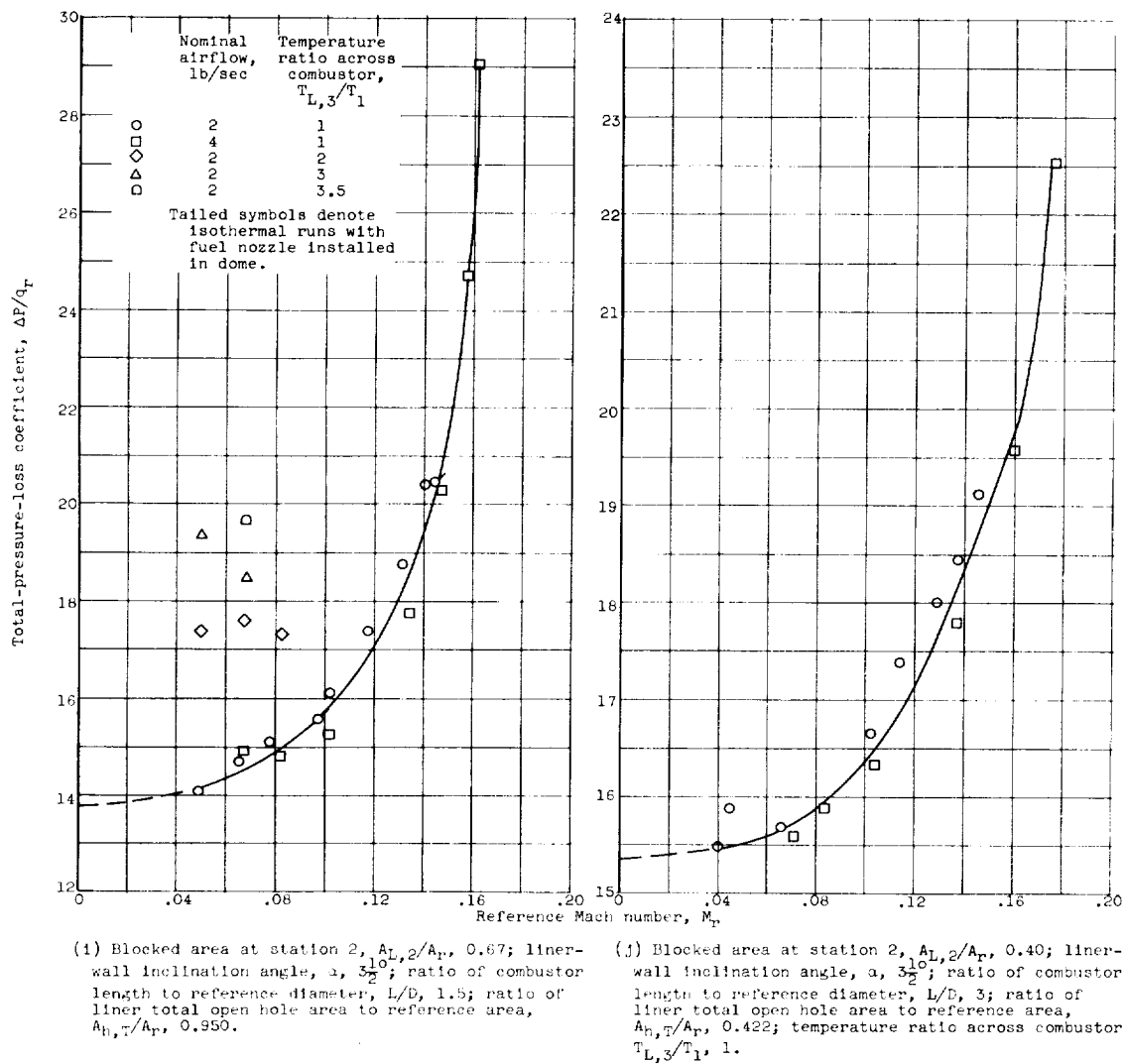
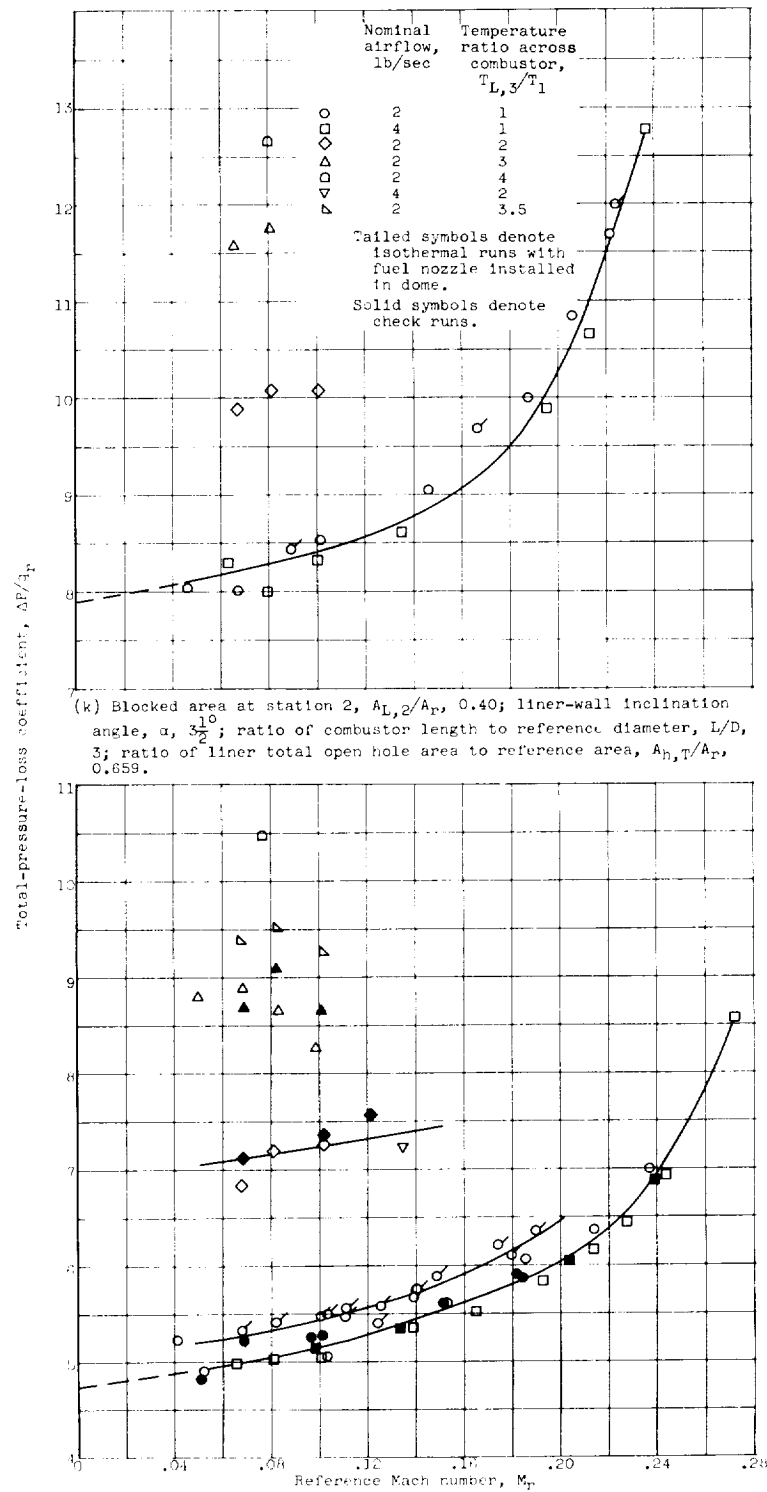


Figure 11. - Continued. Variation of experimental total-pressure-loss coefficient with reference Mach number for 12 tapered liners.

E-126

CQ-6



(k) Blocked area at station 2,  $A_{L,2}/A_P$ , 0.40; liner-wall inclination angle,  $\alpha$ ,  $3\frac{1}{2}^\circ$ ; ratio of combustor length to reference diameter,  $L/D$ , 3; ratio of liner total open hole area to reference area,  $A_{h,T}/A_P$ , 0.659.

(l) Blocked area at station 2,  $A_{L,2}/A_P$ , 0.40; liner-wall inclination angle,  $\alpha$ ,  $3\frac{1}{2}^\circ$ ; ratio of combustor length to reference diameter,  $L/D$ , 3; ratio of liner total open hole area to reference area,  $A_{h,T}/A_P$ , 0.95.

Figure 11. - Concluded. Variation of experimental total-pressure-loss coefficient with reference Mach number for 12 tapered liners.

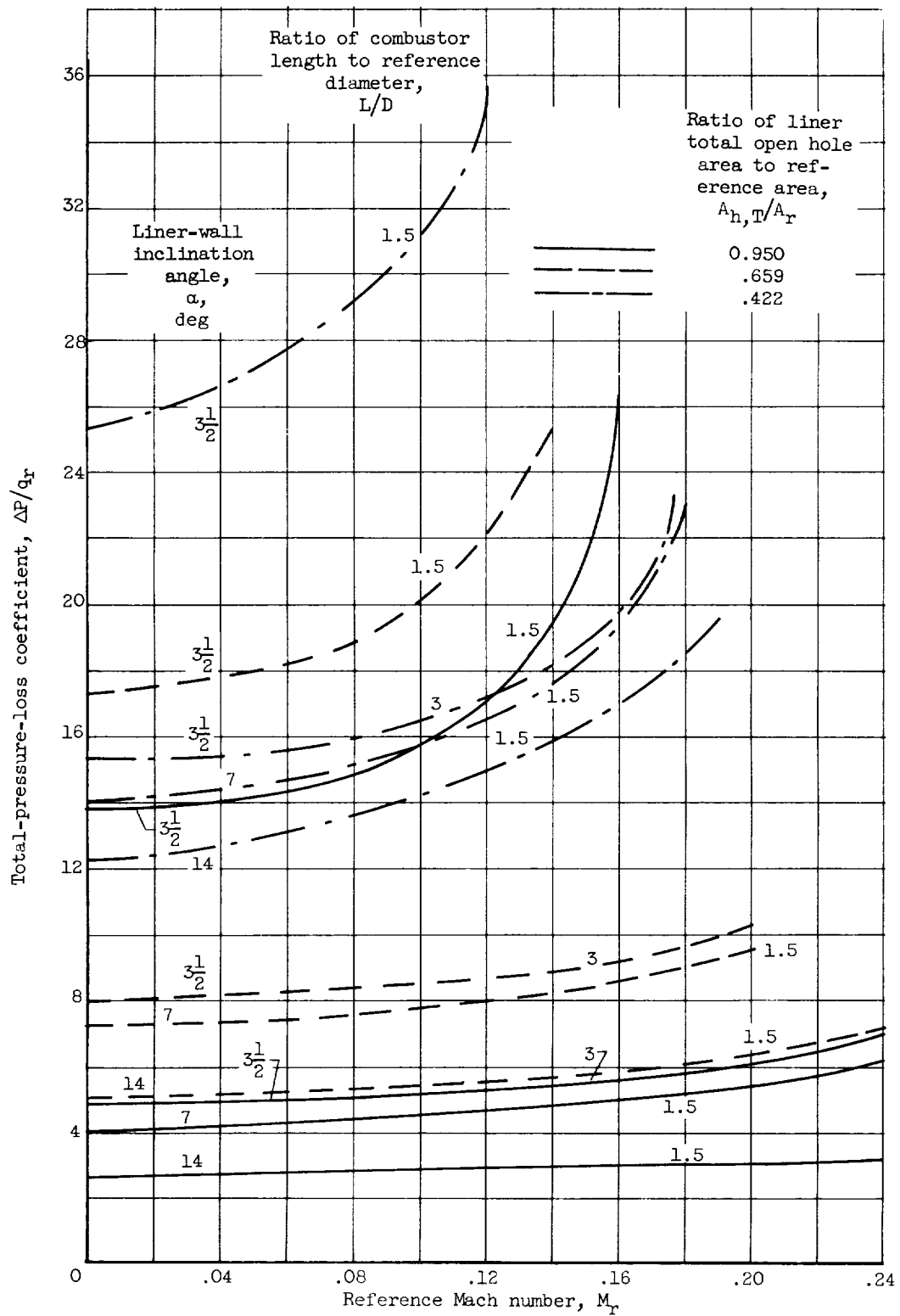


Figure 12. - Comparison of effect of reference Mach number on experimental isothermal total-pressure-loss-coefficient of 12 tapered liners.

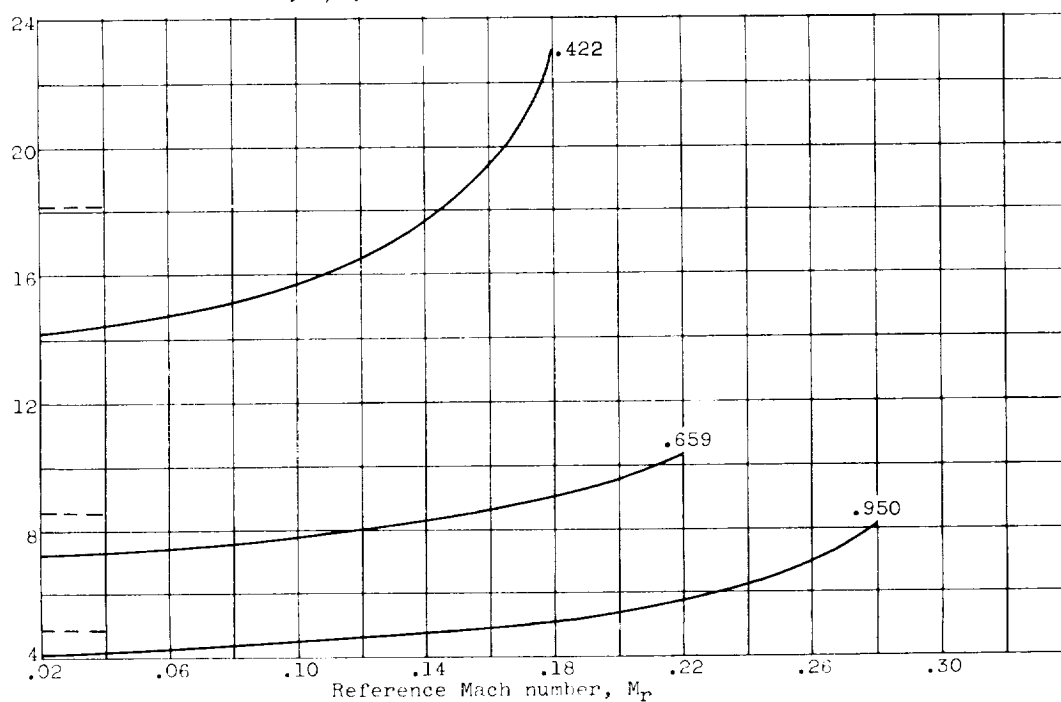
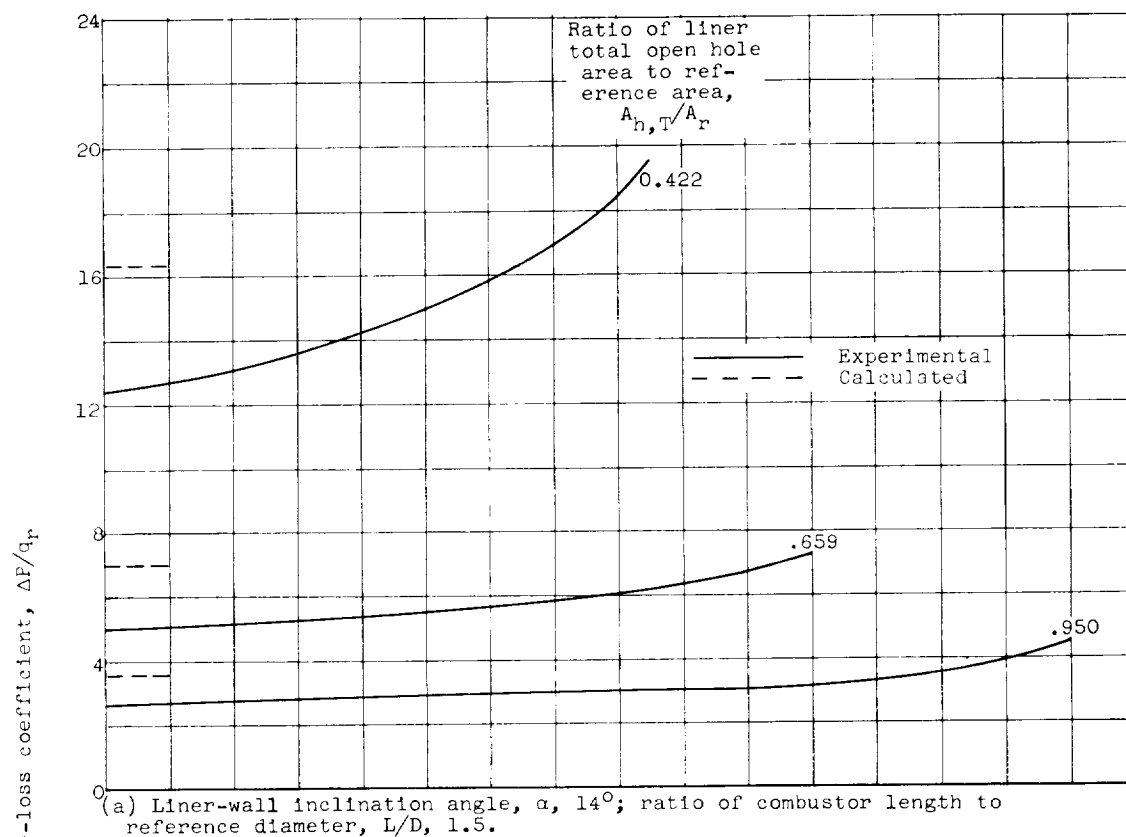


Figure 13. - Comparison of calculated and experimental isothermal total-pressure-loss coefficients of 12 tapered liners.

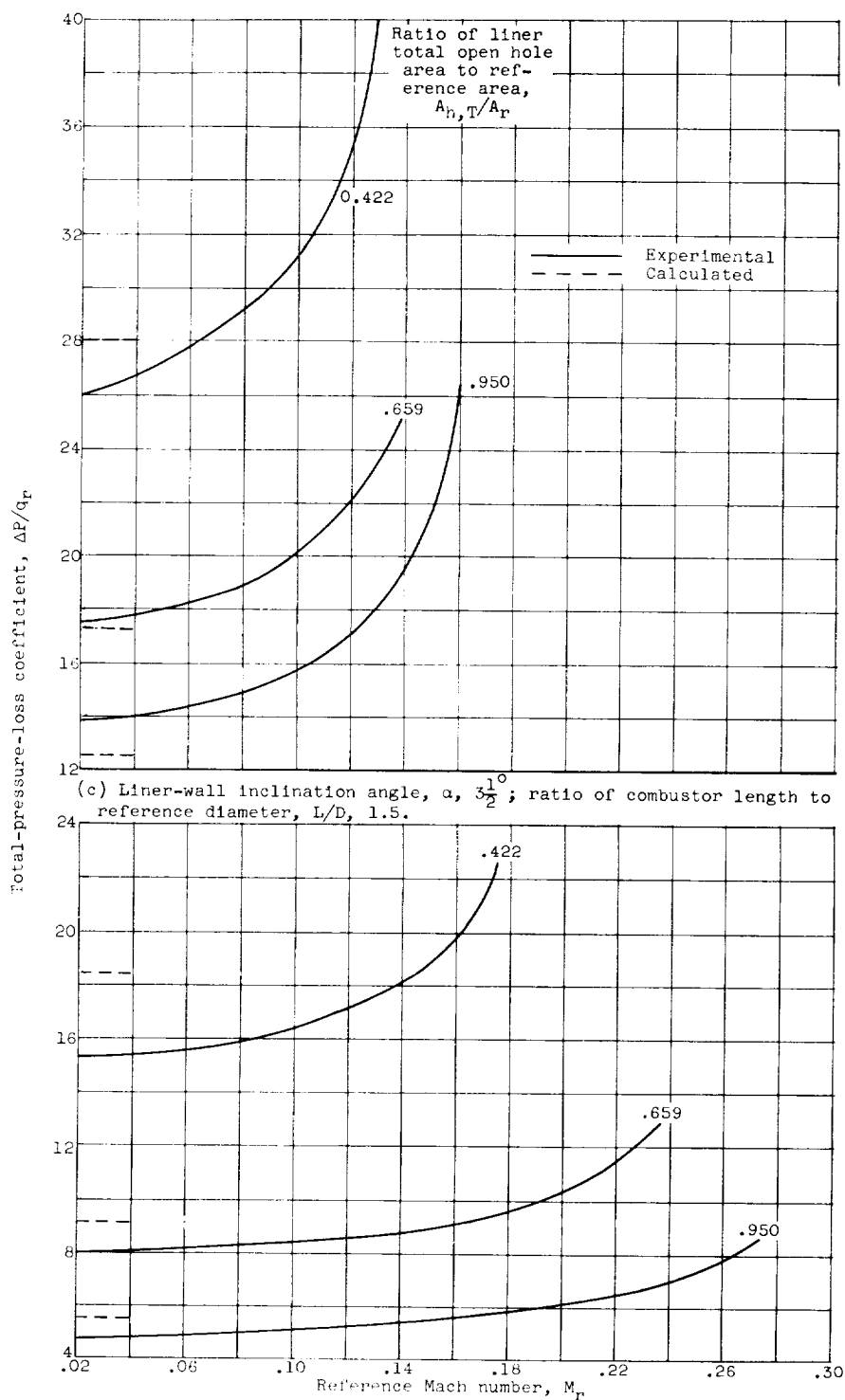


Figure 13. - Concluded. Comparison of calculated and experimental isothermal total-pressure-loss coefficients of 12 tapered liners.

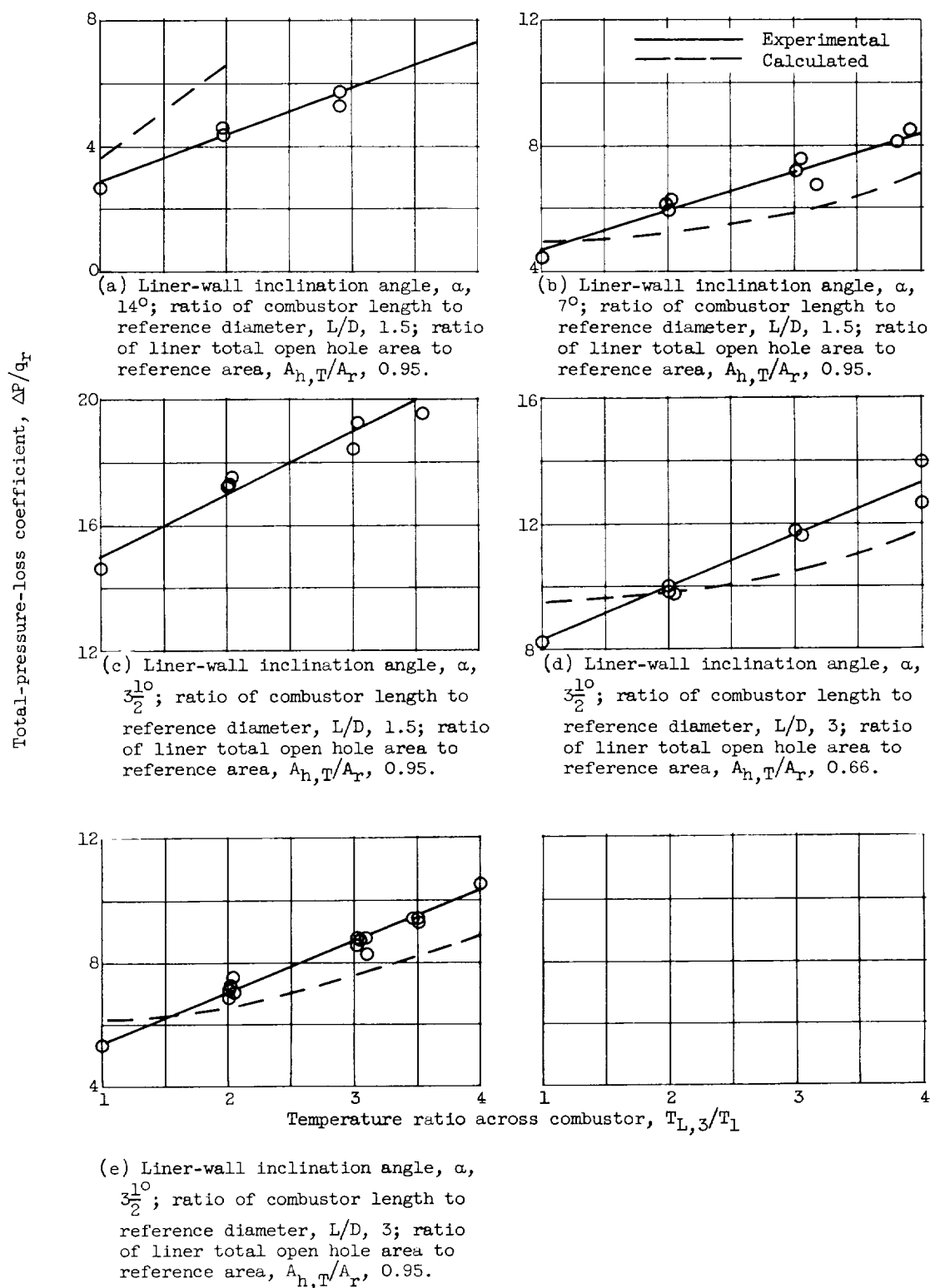


Figure 14. - Comparison of calculated and experimental total-pressure-loss coefficients with heat release for five tapered liners.

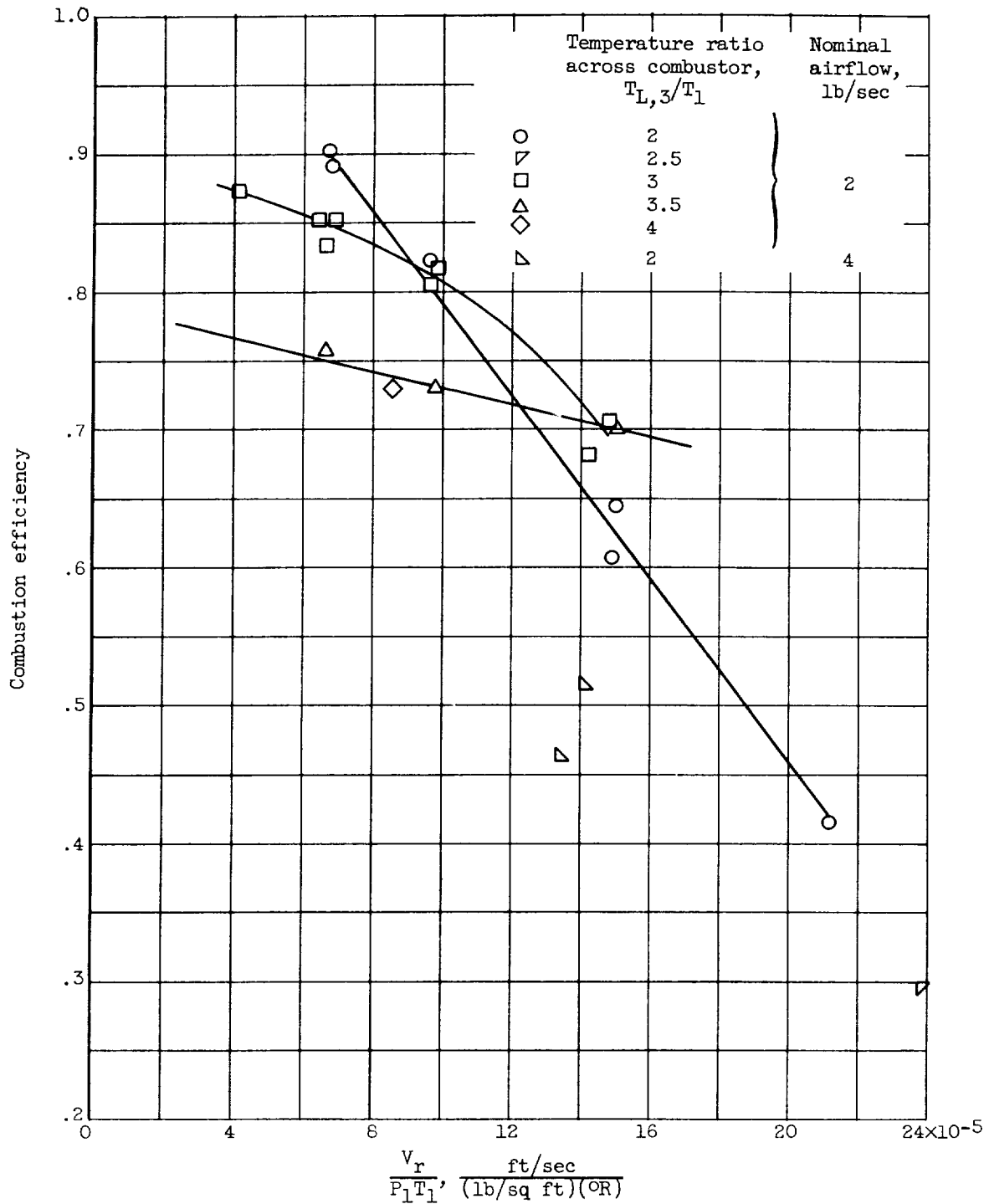


Figure 15. - Variation of combustion efficiency with correlating parameter for one tapered liner. Liner-wall inclination angle,  $\alpha$ ,  $3\frac{10}{2}$ ; ratio of combustor length to reference diameter,  $L/D$ , 3; ratio of liner total open hole area to reference area,  $A_{h,T}/A_r$ , 0.95.



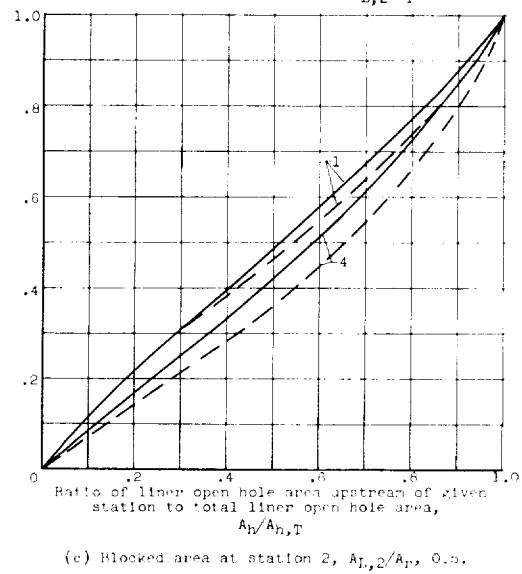
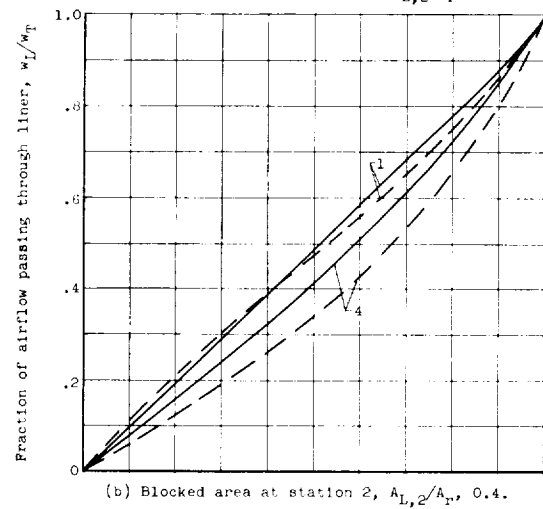
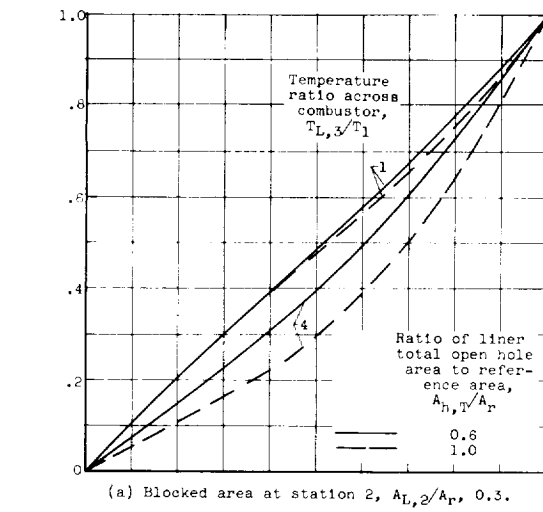


Figure 16. - Effects of total open hole area and temperature ratio on liner airflow distribution.

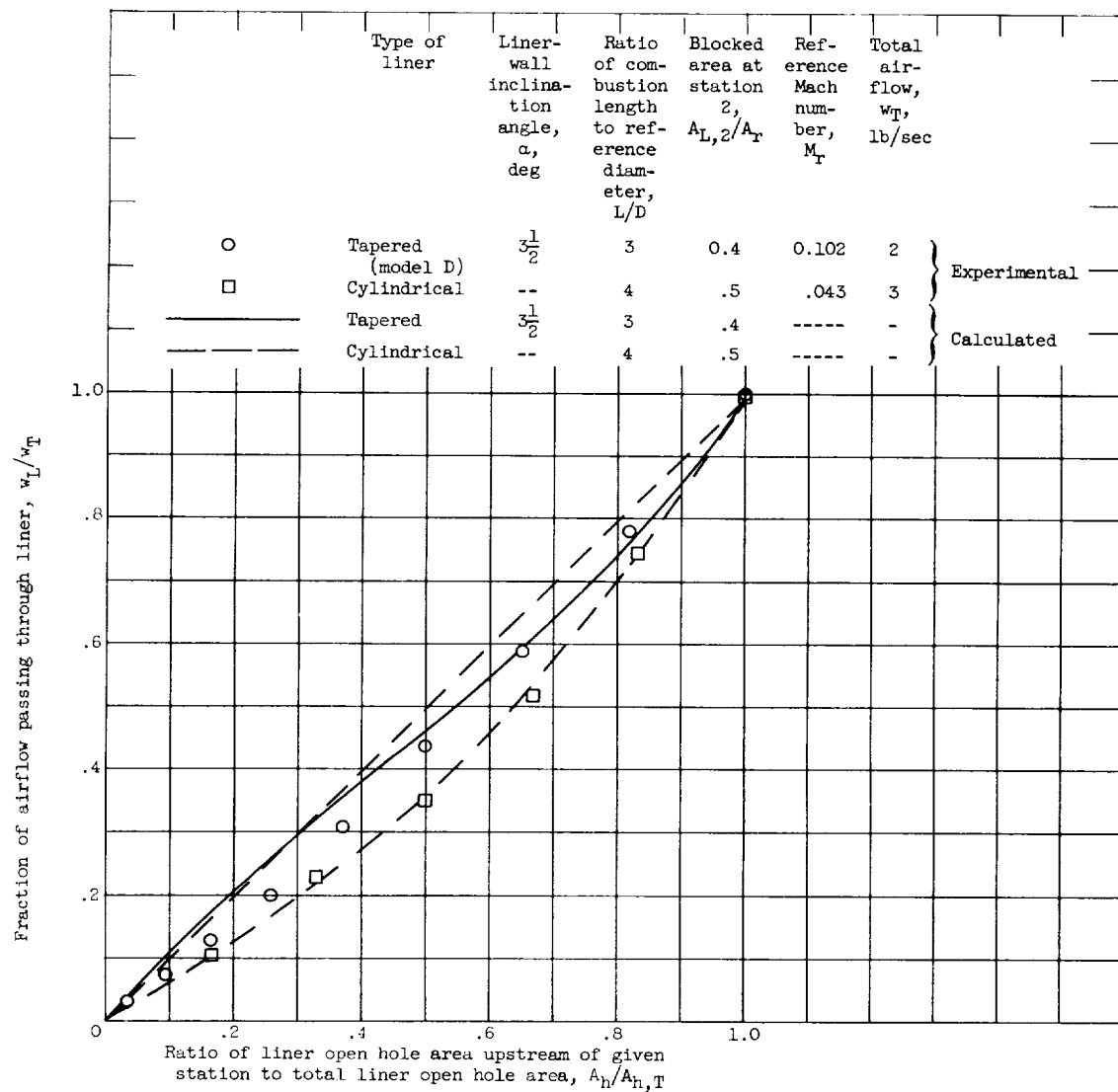


Figure 17. - Comparisons of calculated and experimental airflow distributions for one tapered liner and one cylindrical liner. Ratio of liner total open hole area to reference area,  $A_{h,T}/A_R$ , 0.95; temperature ratio across combustor,  $T_{L,3}/T_1$ , 1.